Physics – Uspekhi **51** (2) 133 – 161 (2008)

REVIEWS OF TOPICAL PROBLEMS PACS numbers: 78.55.Ap, **81.07. – b**, **81.16. – c**

Extremely dense arrays of germanium and silicon nanostructures

A A Shklyaev, M Ichikawa

DOI: 10.1070/PU2008v051n02ABEH006344

Contents

Abstract. Results of investigations into surface processes of the formation of germanium and silicon nanostructures are analyzed. A mechanism of three-dimensional island nucleation and relaxation of strained two-dimensional layers in heteroepitaxy of germanium on silicon, which initiates spontaneous island growth, is considered. The oxidation of the silicon surface prior to germanium or silicon deposition drastically alters the growth mechanism, leading to the formation of islands with an extremely high areal density of $10^{12} - 10^{13}$ cm^{-2} and with sizes of less than 10 nm. The effects of spatial quantization determine their properties. Moreover, arrays of these islands form a unique surface for the growth of Si layers that are able to emit photons in the 1.5 – 1.6-μm wavelength range.

A A Shklyaev Institute of Semiconductor Physics,
Siberian Branch of the Russian Academy of Sciences,
prosp. Akad. Lavrent'eva 13, 630090 Novosibirsk, Russian Federation
Tel. (7-383) 330 85 91. Fax (7-383) 333 27 71
E-mail: shklyaev@thermo.isp.nsc.ru
Quantum-Phase Electronics Center, Department of Applied Physics,
University of Tokyo and Japan Science and Technology Agency, CREST
7-3-1 Hongo, Bunkyo-ku, Tokyo 113-8656, Japan
Tel./Fax +81 3 5841 7903. E-mail: shklyaev@exp.t.u-tokyo.ac.jp
M Ichikawa Quantum-Phase Electronics Center,
Department of Applied Physics,
University of Tokyo and Japan Science and Technology Agency, CREST
7-3-1 Hongo, Bunkyo-ku, Tokyo 113-8656, Japan
Tel./Fax +81 3 5841 7901. E-mail: ichikawa@ap.t.u-tokyo.ac.jp

Received 1 February 2007, revised 21 June 2007
Uspekhi Fizicheskikh Nauk **178** (2) 139 – 169 (2008)
DOI: 10.3367/UFNr.0178.200802b.0139
Translated by E Yankovsky; edited by A Radzig

1. Introduction

Fabricating semiconductor structures with new physical properties constitutes the main goal of nanotechnology, which aims at expanding the limits of application of semiconductor materials [1 – 4]. The key area of research here is the miniaturization of the structures being created to sizes at which the effects of spatial quantization substantially change the electronic properties of the structures. Special attention is focused on silicon-based structures which constitute the element base of most modern electronic devices. The discovery of new physical properties in such cases makes it possible to build new devices by using the well-developed techniques of silicon microelectronics. An important problem that has yet to be solved is the fabrication of silicon and silicon/germanium structures with an effectiveness of optical transitions sufficiently high for use as radiation sources. The increase in effectiveness is possible thanks to spatial quantization effects. For these effects to manifest themselves, the geometric dimensions of the nanostructures must be about 10 nm or smaller [1, 3]. Moreover, the density of arrays of such structures must be as high as possible.

The methods of fabricating dense arrays of three-dimensional nanoislands on semiconductor surfaces are usually based on the process of self-organization in the epitaxial growth of stressed heterostructures [1 – 6]. The mechanical stress that emerges because of the mismatch in the lattice constants of the growing layer and the substrate causes a transition from two-dimensional layer growth to the formation of three-dimensional islands. This mechanism has been used to fabricate various nanostructures for many semiconductor materials. The same approach has been implemented

in heteroepitaxy of germanium on silicon [2, 6]. In the case of germanium deposition on the Si(001) surface at about 500 °C, the two-dimensional growth of the wetting layer is replaced by the formation of three-dimensional islands, often referred to as hut clusters [7, 8]. These islands have the smallest sizes among three-dimensional germanium islands fabricated on silicon surfaces in the Stranski – Krastanov (SK) growth regime. However, even the smallest of these islands are no smaller than 20 nm at their base.

In the current review we use the example of germanium growing on the Si(111) surface to analyze the situation in which the formation of islands smaller than 10 nm is impossible when the passage from two-dimensional to three-dimensional growth in the SK regime is employed. The reasons stem from the kinetic factors determining the nucleation mechanism of the three-dimensional islands in the supersaturated layer of adatoms on the surface of the elastically strained two-dimensional germanium layer. The relaxation of the surface after nucleation of the islands causes them to spontaneously grow to sizes much bigger than 10 nm.

The limited possibilities of the effect on the spontaneous growth of the islands by selecting the proper experimental conditions prompted the development of new methods based on the modification of the initial silicon surface. For instance, deposition on the silicon surface of such materials as carbon and arsenic in quantities amounting to one monolayer significantly alters the mechanism of subsequent germanium growth and makes it possible to fabricate islands smaller than 20 nm at the base, with the density of their arrays being about 3×10^{11} cm^{-2} [9] and 5×10^{11} cm^{-2} [10], respectively. The strongest changes in the growth mechanism have been observed when the silicon surface was oxidized prior to germanium deposition. In this case, germanium growth begins together with the nucleation of three-dimensional islands (without formation of a wetting germanium layer) with an exceptionally high density of their arrays (about 2×10^{12} cm^{-2}) and a size down to 10 nm [11]. The mechanisms underlying this process are discussed in detail in the review.

The homoepitaxial growth of silicon occurs layer by layer due to the movement of the atomic steps either initially present on the surface or forming anew as a result of the nucleation of two-dimensional islands on atomic-step terraces [12 – 14]. This mechanism is used to create quantum wells and superlattices by growing δ-doped silicon layers in the silicon matrix [15], together with various surface phases [16]. As silicon grows on silicon, no new elastic strains in the lattice appear, which means there are no conditions for the formation of three-dimensional islands. The use of oxidized silicon surfaces is necessary for the formation of such islands. Three-dimensional silicon islands nucleate on an oxidized surface with an array density higher than that of germanium islands. What is interesting is that at temperatures close to 640 °C and higher the silicon oxide film is completely desorbed from the surface in the course of island growth, while three-dimensional silicon islands themselves form on the surface at higher temperatures as well [17]. The use of an oxidized silicon surface makes it possible, in principle, to create doped islands of silicon in the silicon matrix if the doping happens in the growth process at the stage when three-dimensional islands are formed.

The role of mechanical stresses in the formation of 10-nm nanostructures (or even smaller) is insignificant compared to the kinetics of direct interatomic interactions and the formation of local interatomic bonds. Surface diffusion, island nucleation, and the incorporation of deposited atoms into preferable sections of the surface in order to ensure its selective growth are the decisive processes here. The reactions between the deposited atoms and intermediate coatings that create conditions needed for island nucleation are important only in the very first stage of growth. The hemispherical shape of forming islands with sizes up to 10 nm serves as an indication that neither the crystalline silicon substrate nor the forces causing facet formation by dint of energy-advantageous planes produce a profound effect on it. Faceting is observed only in silicon islands with sizes of about 10 nm and larger, grown at temperatures above 570 °C, when the amount of remnants of the silicon oxide film on the surface is insignificant [17].

An oxidized silicon surface covered by a mixture of epitaxial and nonepitaxial three-dimensional islands of germanium or silicon is unique for subsequent growing silicon layers on it. The deposition of silicon atoms leads to a continuation of growth of three-dimensional islands and to their coalescence. In the process, a layer containing areas of silicon with a high concentration of stacking faults forms. High-temperature annealing forms nanostructured silicon which consists of crystal silicon clusters separated by sections with a system of crystal defects that act as quantum wells with a narrower forbidden band (about 0.8 eV). Such silicon layers are capable of effectively emitting light in the 1.5 to 1.6-μm wavelength range [18] which is widely used in fiber-optical communication lines.

The formation of germanium and silicon nanostructures with sizes in the 1 – 100 nm range has been studied with a molecular beam epitaxy (MBE) facility equipped with instruments for scanning reflection electron microscopy (SREM), scanning tunnel microscopy (STM), and high-energy electron diffraction (HEED). The design of the facility made it possible to take images of the surface by all these methods simultaneously during layer growth, and to study them by the energy-dispersive X-ray (EDX) spectroscopy after the growth terminated. Silicon nanostructures were grown in a separate chamber in order to study them by the low-energy electron diffraction (LEED) method and by electron energy loss spectroscopy. Nanostructures on large-sized silicon substrates were grown in another specially designed MBE device for further studies by photoluminescence (PL) and electroluminescence methods, by spectroscopy of the fine structure of the X-ray absorption edge, and by transmission electron microscopy (TEM).

2. Self-organization of germanium layers on Si(111)7 × 7 surfaces

The growth of germanium on silicon is accompanied by the emergence of elastic strains caused by the mismatch in the lattice constants of the substrate and the growing layer. Partial reduction in these strains occurs because of the transition from layer growth to the formation of three-dimensional islands [7, 19 – 23]. Heteroepitaxial growth with such a transition is known as the Stranski – Krastanov regime. What is important here is that a reduction in strains may occur without the introduction of dislocations [21, 24, 25]. Spontaneous formation of three-dimensional islands during the transition from two-dimensional growth to three-dimensional growth was employed as a unique mechanism for

fabricating nanostructures [1–8, 24, 26, 27]. As germanium grows on silicon, rather large islands form, with sizes at the base varying from 30 to 100 nm on Si(111) surfaces [23, 28], and from 30 to 600 nm on Si(001) surfaces. Germanium islands on Si(111) tend to become more ordered during growth [30, 31]. Furthermore, it has been found that the size and shape of the forming islands are temperature-dependent [7, 24, 32–34]. The presence of a temperature dependence is an indication that the kinetics of surface processes has a marked influence on the formation of the surface morphology during growth. Understanding its role in the self-spontaneous formation of islands is necessary in order to fabricate nanostructures of given sizes.

The spontaneous formation of islands has been thoroughly studied and theoretically described in terms of minimization of the free energy comprising the strain energy for cases where the growing layers acquire a thermodynamically equilibrium morphology irrespective of the values of the kinetic parameters for surface processes during growth. For the case of germanium on silicon, the constructed elastic-stress distribution models predict a regular arrangement of germanium three-dimensional islands spaced approximately 100 nm apart both in the lateral direction and in the direction of growth in the fabrication of multilayer structures [35–37]. However, the theoretical models require the formal introduction of additional parameters accounting for the mechanism of formation of surface structures with smaller characteristic spacings. Such a case involves, for instance, surfaces covered by hut clusters of germanium on Si(001) and their evolution to an equilibrium form consisting of large pyramidal and dome-shaped islands [36].

Another approach to describing the formation of islands consists in using a theory of reaction rates that describes the interaction of surface atoms [38–41]. Such an approach does not predict the very fact of transition from two-dimensional growth to three-dimensional growth, but its application is justified when the kinetic parameters of the processes of nucleation and growth of three-dimensional islands play a significant role in the mechanisms that form the surface morphology. Generalized experimental information about the surface processes is contained in the dependences of island density on the growth temperature, the deposition rate, and the coating size [42].

Earlier research has shown that germanium growth on the Si(111)7 × 7 surface begins with the formation of the two-dimensional layer which is subjected to reconstruction with a 5 × 5 superstructure at coatings of about two bilayers (BLs) [1 BL = 2 monolayers (ML) ≈ 1.57×10^{15} atoms per square centimeter on Si(111)]. The transition from two-dimensional growth to three-dimensional growth occurs when the coatings range between 2 and 3 BLs, depending on the growth temperature [20, 22, 28]. A characteristic feature of this transition is that three-dimensional islands appear more or less suddenly [22, 28], with the shape of the islands being that of truncated tetrahedral pyramids with {113} faces on the lateral sides [22]. This shape of islands has been observed at growth temperatures ranging between 350 and 450 °C [28]. Thicker germanium coatings are characterized by the formation of islands that are bigger but exhibit a flat top having a (111) orientation with a 7 × 7 superstructure [22]. It should be noted that other faces have also been observed on the lateral sides of the islands, such as {133}, {112}, and {122}, which formed on large flat islands after deposition of 25 BLs [20]. In this section we shall present data on the nucleation and growth of three-dimensional germanium islands on the Si(111) surface at coatings close to the transition from two-dimensional growth to three-dimensional growth.

2.1 Size and number density of islands

Figure 1 shows SREM images of a surface covered with 3.5 BL of germanium at three temperatures. The island shape depends on the growth temperature [34]. We call the pyramidal-shaped islands with {113} facets on the lateral sides [27] high islands to distinguish them from flat islands which form at higher temperatures. The high islands look like tops in the SREM images (see Fig. 1b), and the reason is that the SREM method relies on a glancing angle of incidence of the electron beam on the silicon surface, with the image of an island consisting of a real upper part and its shadow which is the lower part of the image. High islands form on the surface at temperatures ranging from 380 to 450 °C (Fig. 1a). Simultaneous formation of high and flat islands is observed in the medium temperature range extending from 450 to 580 °C (Fig. 1b). Flat islands with large base sizes form at temperatures above 580 °C (Fig. 1c). The surface between the islands undergoes reconstruction with a 5 × 5 superstructure [34], which is typical of pseudomorphic germanium layers on the Si(111) surface [22]. Figure 1d demonstrates that the island number density N changes by a factor of approximately 1000 as the temperature grows from 380 to 690 °C. Notice that at low and high temperatures the slopes of the temperature curve differ slightly.

Information about the process of island nucleation is contained in the form of the dependence of the island number density on the flux F of the atoms impinging on the surface. Figure 2 shows that the island number density is much higher when the flux of germanium atoms falling on the surface is higher. Here, the high-to-flat island number ratio does not depend on F. The dependence of the island number density on flux was measured for two temperatures [Fig. 2c; also see formulas (1)–(3) below]. The approximation of these data by a power function produced the following values of the exponent: $p \approx 0.77$ and 0.79 ± 0.01 for 480 and 580 °C, respectively [34]. The difference in the values of the exponent shows that the size of the critical islands increases at higher growth temperatures. This result agrees with the slope of the temperature curves for the island number densities in Fig. 1d, where the larger slope at the higher temperature corresponds to the more sizable critical islands.

Since flat islands and high islands form simultaneously in a broad temperature interval, the possibility of their transformation from one form into the other under annealing was checked. It was found that the shape of islands does not change under annealing. It must also be noted that single atomic steps on the initial silicon surface have no influence on the nucleation probability or the shape of germanium islands. STM was used to establish that high islands slightly change their shape as they grow in such a way that the geometric factor (the ratio of an island's height to its length at the base) decreases [28]. The above data indicate that no differences in the nucleation of high islands and flat islands have been found and that the distinctions in their shape appear in the growth stage.

The island number density reaches saturation in a short time interval after the emergence of the first islands (Fig. 3). At a germanium atomic flux of about 0.24 BL min^{-1}, the island number density reached saturation in the coating-thickness interval from 3.0 to 3.1 BL at growth temperatures

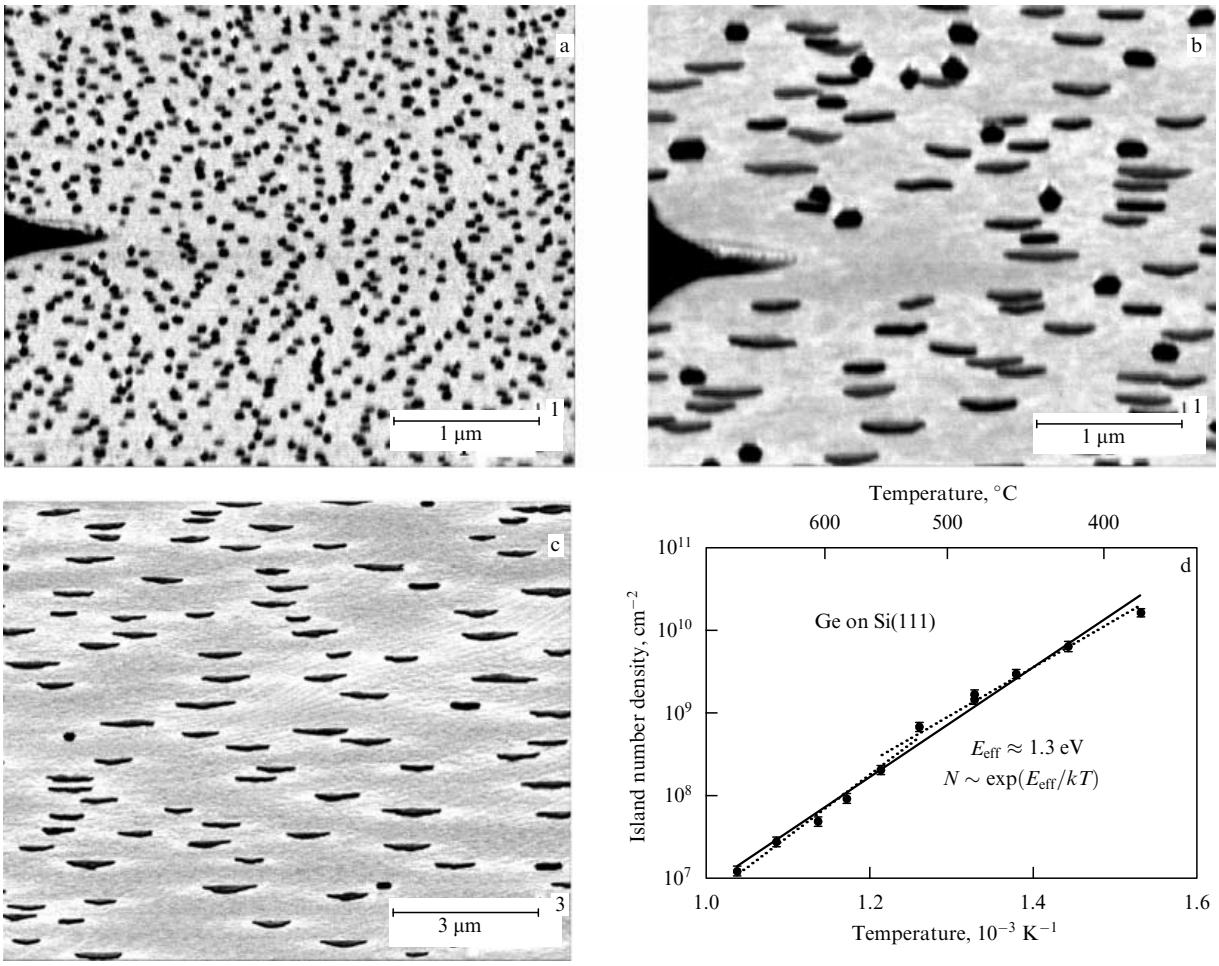

Figure 1. SREM images of an Si(111) substrate covered with three-dimensional germanium islands fabricated after deposition of 3.5 BL of germanium with a rate of 0.24 BL min^{-1} at 420 °C (a), 500 °C (b), and 580 °C (c). (d) The respective temperature dependence of the number density of three-dimensional germanium islands. The solid line represents the approximation of the experimental data by a single exponential function in the entire temperature range. The dotted lines represent separate approximations for the high- and low-temperature domains.

below 500 °C [34]. This observation agrees with the results of other investigations in which the emergence of three-dimensional islands was characterized as sudden [22, 28]. Thus, the dependences of the island number density on temperature and atomic flux, shown in Figs 1d and 2c, respectively, were obtained for islands with saturated number density. This fact was taken into account in selecting an appropriate theoretical model for describing the nucleation of islands.

2.2 Critical size of islands

The theory of nucleation and growth of islands on the crystal surface has found successful application in cases where the islands of critical sizes are small, e.g., consist of several atoms. The main theoretical result which is usually used for analyzing the experimental data lies in the derivation of simple relations between the number density of stable islands and the growth parameters, such as the magnitude of the impinging atomic flux, the size of a 'critical' island, the surface diffusion coefficient, and the energy needed to detach one atom from an island of critical size [38 – 41]. These relations have been derived for several possible cases of the early crystal growth stage. The size of a critical island is the key parameter of the theory and characterizes the growth process as follows. The emergence of islands reduces the concentration of adatoms on the surface because they are spent in growing the nucleating islands. If island nucleation occurs only in the initial stage of growth, the nucleation process is extremely sensitive to adatom concentration. This becomes possible when the critical island is sizable, so that the reduced adatom concentration is not high enough for new nuclei of critical size to form. When the critical islands are small, a high concentration of adatoms is not needed for their nucleation. Then, the probability of small islands forming on the surface is substantial even if the adatom concentration is reduced. The growth of germanium on the Si(111) surface is characterized by the sudden emergence of islands [22, 28] with a number density corresponding to saturation (see Fig. 3) [34]. This is an indication that critical islands are relatively large.

The following expression for the island number density has been obtained in the context of the theory of reaction rates [39 – 41]:

$$N \sim \left(\frac{F}{D}\right)^{p} \exp\left(\frac{pE_i}{kT}\right), \qquad (1)$$

where F is the flux density of atoms impinging on the surface, D is the adatom diffusion coefficient, E_i is the work performed in the dissociation of a critical island into separate

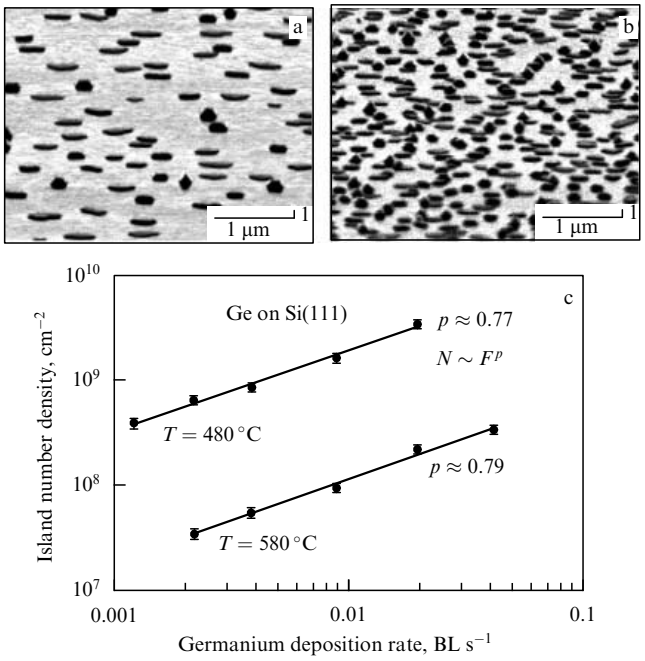

Figure 2. SREM images of a surface with germanium 3D islands grown on Si(111) at 480 °C for two values of the germanium flux: 0.06 BL min^{-1} (a), and 0.6 BL min^{-1} (b). (c) The dependence of the island number density on the flux density F of germanium atoms. Germanium was deposited before coating the surface with 3.5 BL at 480 and 580 °C.

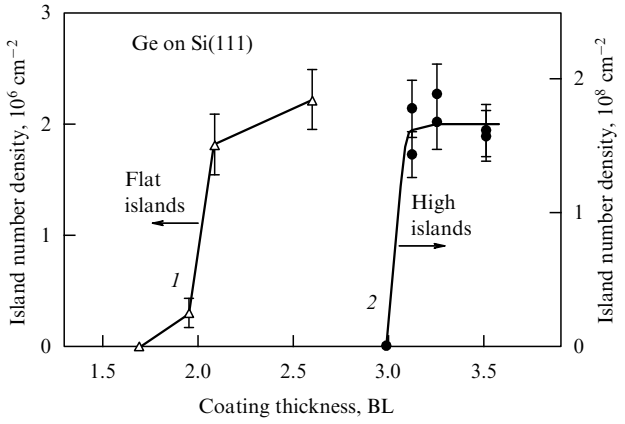

Figure 3. Island number density as a function of coating thickness: *1* — large flat islands that appeared after deposition of a two-dimensional germanium layer at 480 °C and subsequent annealing at 700 °C, and *2* — high islands formed as a result of germanium deposition with a flux density of 0.24 BL min^{-1} at 480 °C. The experimental errors in the figure reflect the difference in island number density for different sections of the surface.

adatoms, and the exponent p is a function of the growth parameters, such as the dimensionality of the nucleating islands and the number i of atoms in the island of critical size. To determine the size of critical islands from the experimental data, one can apply the following relation linking N to F:

$$N \sim F^p \,. \tag{2}$$

As we have shown earlier, the dependence of the island number density N on the atom flux density (Fig. 2c) was obtained for N at saturation and at the growth stage far from the onset of island coalescence. This corresponds to the quasistationary regime, and for the case of total condensation with the formation of three-dimensional islands, the exponent p was obtained in the form [39, 40]

$$p = \frac{i}{i + 2.5} \,. \tag{3}$$

With the data presented in Fig. 2c, formula (2) yields the averaged size of critical islands, which amounts to 8.4 and 9.4 ± 0.5 atoms at 480 °C and 580 °C, respectively. This result indicates that for critical germanium islands on Si(111) the number i of atoms slightly grows as the temperature increases. Such temperature behavior of i is quite common [43–45], since at higher temperatures the critical islands of larger sizes are required because they are more stable. Although Markov [41] doubted that expressions of type (3), usable for large critical islands, could be employed in describing the formation of two-dimensional islands, in our case the possibility of great i's agrees on the qualitative level with the following features of the growth process. Island nucleation begins only after a supersaturated two-dimensional germanium layer about 3 BL thick has been formed (see Fig. 3) [22, 34]. Below we shall show that this two-dimensional layer partially decays after nucleation of three-dimensional islands. Moreover, islands with a number density corresponding to saturation (see Fig. 3) [46] emerge suddenly in the course of germanium deposition [22, 28]. Large critical islands are bound to form if the pre-exponential factor entering into the rate constant of nucleation is small, which may be due to substantial structural transformations in the transition from two-dimensional growth to three-dimensional growth. Notice that Voigtländer et al. [47] found that the size of critical islands must amount to about six atoms for the nucleation of germanium two-dimensional islands to occur as silicon grows on Si(111). The researchers assumed that such critical islands are needed for a bilayer to emerge, while nucleation of monolayer islands in the epitaxy of silicon on Si(001) requires the presence of much smaller critical islands. The size of critical islands of about nine atoms was determined for the growth of germanium on Si(111) from GeH_4. Here, stable clusters of 10 atoms in size were observed by Rauscher et al. [48], who used STM.

The above results agree with the following scenario of the transition from two-dimensional growth to three-dimensional growth. As the thickness of the two-dimensional germanium layer is built up to 3 BL, elastic strains may reach such a magnitude that the process of incorporating adatoms into the two-dimensional layer becomes disadvantageous in energy. As a result, the adatom concentration rises and the formation of sizable nuclei is made possible. These nuclei grow as three-dimensional entities, since two-dimensional growth is at a disadvantage energywise. After nucleation of the islands, the adatom concentration drops because adatoms are spent in growing the islands, and no new islands nucleate.

The energy characteristics of the surface processes that take place during nucleation of germanium islands can be estimated from the temperature dependence of the island number density. In our case, the following relationship is valid:

$$N \sim \exp\left[\frac{E_i + iE_d}{(i + 2.5)kT}\right], \tag{4}$$

where E_i is the work that must be done to dissociate an island of critical size into separate adatoms, and E_d is the activation energy of germanium adatom diffusion. In what follows we ignore the small increase in the critical size of an island with a rise in temperature and assume that $i = 9$ in the entire temperature range being investigated. The description of the temperature dependence of the island number density by the relation $N \sim \exp(E_{\text{eff}}/kT)$ yields $E_{\text{eff}} = 1.3$ eV, as shown in Fig. 1d. If $\Delta E_i = E_i - E_{i-1}$ is the work that must be done to detach one atom from an island of size i, we may assume that for large islands ΔE_i is independent of i and that $E_i = i\Delta E$. Taking this assumption into account, we see that equations (3) and (4) yield

$$(\Delta E + E_d)\, p = E_{\text{eff}}\,. \tag{5}$$

The activation energy needed for germanium adatom diffusion over the Ge(111)c(2 × 8) surface was evaluated theoretically by Selloni et al. [49]. The researchers found that the most preferable track that diffusion takes involves two states whose potential energies differ by approximately 0.6 eV. What is more, as an atom follows this track, it surmounts a 0.2-eV potential barrier. The sum is a diffusion activation energy of about 0.8 eV [49]. Using this value for E_d and assuming that $p \approx 0.78$ (Fig. 2c), we determine from equation (5) that in our case $\Delta E \approx 0.9$ eV. The corresponding activation energy of detaching one germanium atom from an island [with allowance for the fact that the atom must surmount an energy barrier of about 0.2 eV ($E_{\text{det}} = \Delta E + 0.2$ eV)] amounts to 1.1 eV. Notice that this magnitude of the activation energy is close to 1 eV, which is the value obtained in experiments involving a field ion microscope [50, 51] and LEED [52] for the Ge(111) surface in the process of the surface's relaxation via adatom detachment and diffusion.

The formation of three-dimensional islands reduces the elastic strains in the two-dimensional epitaxial germanium layer on silicon. The shape of the islands can characterize the relaxation mechanism of these strains. For coherently stressed islands, i.e., islands whose emergence reduces the stresses without introducing dislocations, the theoretical model of Spencer and Tersoff [53] predicts that in the ideal case the strain energy is reduced when, as the thickness of the coating increases, the coherent islands acquire the shape of a ball on top of the two-dimensional layer. Such a shape of the islands results in the smallest possible contact with the substrate. In our case, the emergence of high islands with a relatively small area of contact apparently takes place without the production of dislocations [54]. The formation of flat islands with sizable bases at high temperatures may be accompanied by the emergence of a dislocation network [25, 55] at the boundary between an island and the substrate. Notice that in describing the process of island nucleation the researchers used a theory that ignored the energy of lattice elastic deformation. This deformation reduces the work ΔE by an amount equal to the decrease in the strain energy as a result of detachment of a germanium atom from a stressed island.

2.3 Indications of 2D layer decay

In this section we deal with direct indications that two-dimensional germanium layers on silicon surfaces are unstable and partially decay after the nucleation of three-dimensional islands. This decay initiates a spontaneous growth of islands even in the absence of an external flux of germanium atoms. The formation of unstable phases is a general property of the SK growth regime in epitaxy of germanium on silicon surfaces and the reason is the competition between the kinetics of nucleation and growth of islands and the formation of a thermally stable surface morphology.

Figures 4a–c exhibit images of the Si(111) surface covered with three-dimensional germanium islands in the conditions where the heating of the sample was terminated several seconds after deposition of 3.1 BL of germanium ceased. Subsequent annealing of the structure at 480 °C for 10 min leads to a substantial increase in island size, while the number of islands remains the same (Fig. 4b). Additional annealing causes further growth of islands (Fig. 4c). The islands can become bigger in the course of annealings only at the expense of germanium that diffuses to the islands from the surrounding sections of the surface. This means that the two-dimensional germanium layer around the islands becomes thinner. This also means that in the presence of nucleated three-dimensional islands the two-dimensional germanium layer is thermally unstable. Notice that the increase in the size of three-dimensional islands under annealings has also been observed at lower temperatures (at 380 °C, for instance) [46].

The thermal stability of two-dimensional germanium layers depends on the coating thickness. For thicknesses ranging from 2.0 to 2.6 BL, the layers are thermally stable up to 550 °C. After they are annealed, a small number of sizable flat islands are formed at higher temperatures (curve *1* in Fig. 3). The annealing temperature at which three-dimensional islands begin to form decreases as the germanium coating becomes thicker. Figure 4d depicts islands on the surface covered with germanium with a layer thickness of 2.7 BL, obtained after annealing at 510 °C for 15 min. Since the sections of the surface covered with a thicker germanium layer produce a darker field in the SREM images, the presence of light sections around the islands in Fig. 4d indicates that the coating thickness decreases as a result of germanium diffusion to the islands. Subsequent annealing at a higher temperature initiates growth of flat islands to a size of 3 μm at the base and the formation of light and dark bands along the atomic steps (Fig. 4e). The light bands representing a thinner germanium layer are located along the upper edge of an atomic step. Such a structure of the two-dimensional layer is thermally stable. Three-dimensional islands, either high or large flat ones, are also thermally stable and are not transformed into one another under annealings up to 700 °C.

A decrease in the thickness of the germanium layer on the sections of the surface between three-dimensional islands caused by annealings was measured by the EDX spectroscopy method that used an electron beam focused to 4 nm in diameter. From Fig. 4f it follows that the decrease in the thickness of the two-dimensional germanium layer between the islands occurs faster at higher annealing temperatures, with the equilibrium layers being about 2 BL thick. Since at temperatures up to 550 °C islands begin to form on the surface at coating thicknesses of about 3.0 BL, its difference in thickness from the equilibrium layer means that about 1 BL of the two-dimensional germanium layer is spent for the formation of three-dimensional islands [46].

Figure 5 depicts SREM images of germanium layers on the Si(111) surface, which were obtained under different experimental conditions [56]. The image of the two-dimensional germanium layer in Fig. 5a displays lines corresponding to atomic steps and small darker sections on the step terraces, which constitute two-dimensional islands. The

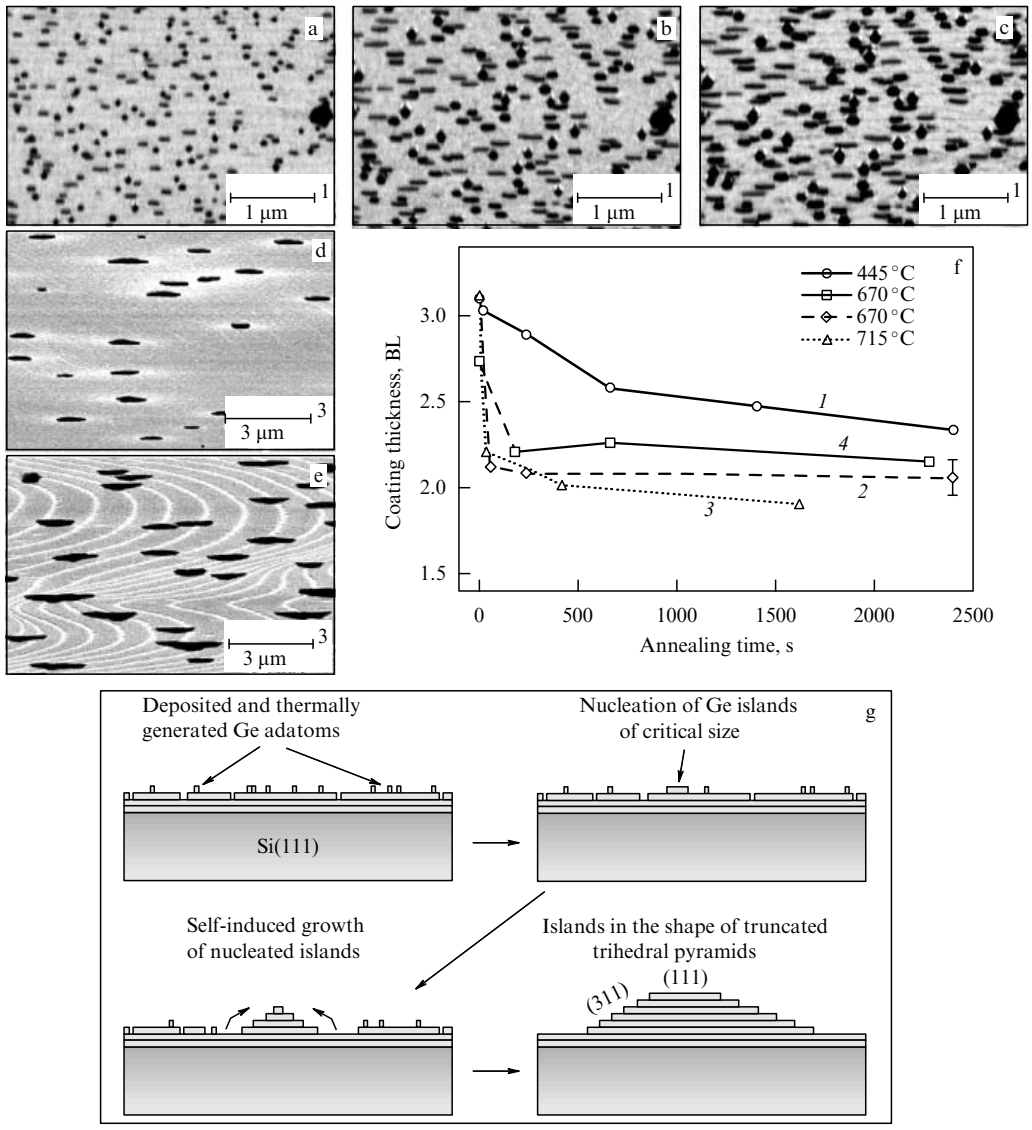

Figure 4. (a, b, c) SREM images of surfaces with three-dimensional germanium islands on Si(111), obtained after the deposition of 3.1 BL of germanium at 480 °C (a) and subsequent annealings at 480 °C for 10 min (b) and 25 min (c). These images show the same section of the surface on which the large island to the right, which is a particle of silicon carbide, is used as a reference mark. (d, e) SREM images of surfaces with sizable flat germanium islands that emerged (d) after the deposition of approximately 2.7 BL of germanium on Si(111) at 510 °C and subsequent annealing at the same temperature for 15 min, and (e) after additional annealing at 650 °C for 10 min. (f) The thickness of the two-dimensional germanium layer between the islands as a function of the annealing time, measured for several annealing temperatures. Curves *1–3* were obtained for surfaces with three-dimensional germanium islands that formed in the course of deposition of about 3.1 BL of germanium, i.e., even before annealing began, at 445 °C (*1*) and 480 °C (*2*, *3*). Curve *4* was obtained for large flat islands that formed as a result of deposition of 2.7 BL of germanium at 480 °C and subsequent annealing at 670 °C for 3 min (corresponding to point $t = 0$). (g) Schematic illustration of the nucleation of germanium islands on Si(111) and their self-induced growth at the expense of absorbing 1 BL of a two-dimensional germanium layer.

thermal stability of the two-dimensional germanium layers deposited at temperatures from 380 to 550 °C depends on the layer thickness. Germanium coatings with a thickness of up to 1.9 BL remain two-dimensional under annealings at 700 °C. The region of coatings is marked I in Fig. 5f. A two-dimensional germanium layer with a thickness of 2 to 3 BL is thermally unstable. The range of annealing temperatures and coatings within which the deposited germanium layer remains two-dimensional after annealing for 10 min is marked II. Annealing at higher temperatures initiates the formation of large flat germanium islands and two-dimensional germanium strips along the atomic steps (Fig. 5b). Line *A* in Fig. 5f, plotted on the growth temperature–coating thickness coordinates, marks the boundary between thermally stable structures and structures that change under annealing. In other words, line *A* gives the value of the lowest temperature at which large flat islands appear on the surface after annealing for 10 min. The surface morphology is the same as in Fig. 5b and is formed when germanium deposition occurs directly under conditions corresponding to region III in Fig. 5f. Line *A* demonstrates that the minimum annealing temperature decreases as the germanium coating thickness increases. This dependence agrees with the data obtained by Marée et al. [20] by the HEED method.

At growth temperatures below 550 °C, three-dimensional germanium islands appear on Si(111) when the germanium coating thickness exceeds 3 BL. Such a coating is shown in Fig. 5f in the form of boundary *B*. The range of conditions

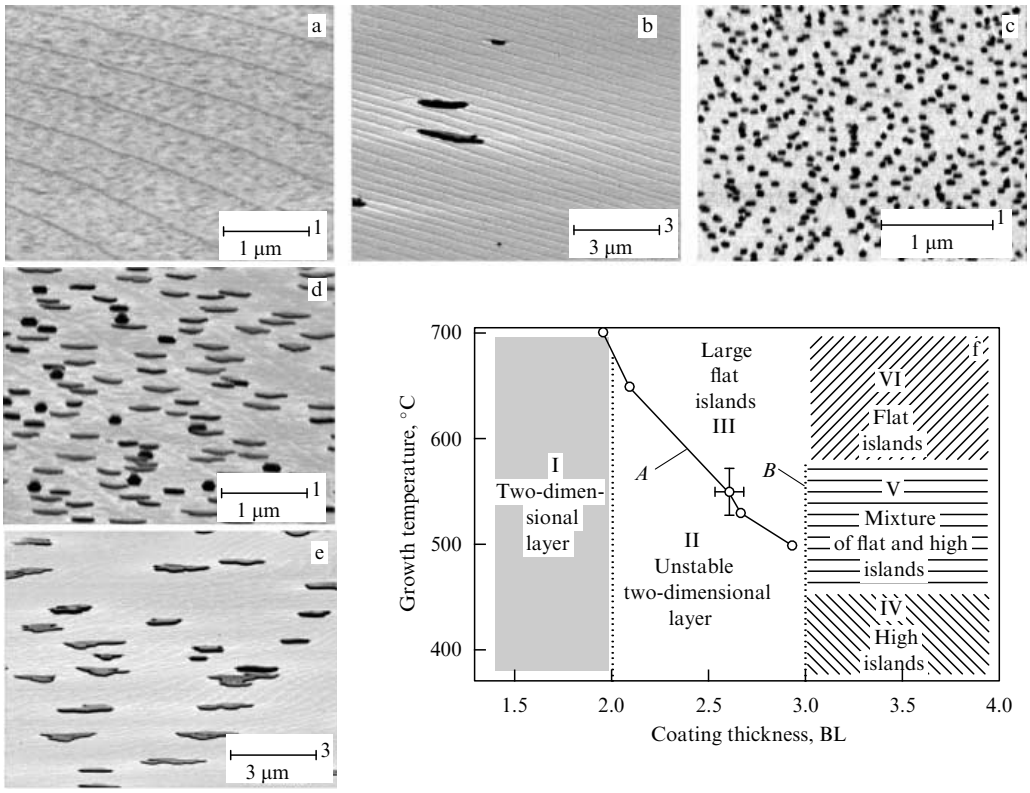

Figure 5. SREM images of germanium layers on Si(111), obtained after deposition of (a) 2 BL at 510 °C, (b) 2 BL at 510 °C and subsequent annealing at 705 °C for 10 min, (c) 3.5 BL at 420 °C, (d) 3.7 BL at 510 °C, and (e) 3.5 BL at 650 °C. (f) Diagram of formation of surface germanium structures on Si(111). The SREM images correspond to the following regions in the diagram: I (a), II (b), IV (c), V (d), VI (e), and III (Fig. 4e). The *A* and *B* lines indicate the boundaries between the regions.

under which only high islands form on the surface is marked IV in this figure. In region V, the high and flat islands coexist. The emergence of large flat islands is predominant at growth temperatures above 580 °C (region VI in Fig. 5f). Notice that the surfaces displayed in Figs 4e and 5e have the same morphology. For this reason, regions III and VI in Fig. 5f are not separated by a continuation of boundary *B* in the high-temperature region. The resulting diagram describes the conditions needed for the formation of various germanium structures on Si(111) as depending on coating thickness and temperature near the transition from two-dimensional growth to three-dimensional growth.

2.4 Self-induced growth of islands after nucleation

The surface morphology created by growth at the expense of germanium atoms supplied by an external source is transformed under subsequent annealings into its equilibrium form. This transformation is caused to a great extent by the generation and diffusion of adatoms. The partial decay of the two-dimensional layer after nucleation of three-dimensional islands is a process similar to what is known as Ostwald ripening, in which the difference in the number density of thermally generated adatoms on the surface sections near small islands and near large islands leads to growth of the large islands, while the small islands become even smaller and finally disappear [57]. The intermediate formation of a thermally unstable two-dimensional germanium layer in our case is probably triggered for the large size of critical islands. In the absence of an external flux of germanium atoms, the number density of the adatoms on the surface, which are thermally generated by the unstable two-dimensional layer, is not high enough for the nucleation of three-dimensional islands to occur with germanium layer thicknesses up to 3 BL and at temperatures of up to 500 °C. For this reason, the development of the surface morphology takes another path under annealing. As is known, misfit dislocations easily form at high temperatures at the boundary between germanium and silicon [58, 59]. Their formation at the island site reduces the elastic strains in it due to the emergence of plastic strain. The reduction in elastic strains opens the possibility for going on two-dimensional growth and leads to the formation of a large flat island [28, 53, 58]. The process does not require that the adatom number density be high and, therefore, may proceed in the absence of an external flux of germanium atoms. In this case, the surface morphology depends neither on the annealing temperature nor on the strength of the atomic flux in the course of germanium deposition.

In Section 2.3 we showed that a two-dimensional germanium layer with a thickness of up to 2 BL constitutes a stable structure on Si(111). It is stabilized by a reconstruction with a 5×5 superstructure. At greater coating thicknesses, the amount of germanium exceeding 2 BL is spent in growing three-dimensional islands after their nucleation (Fig. 4g). At temperatures below 500 °C and coating thicknesses greater than 3 BL, preferably high coherent islands nucleate. Their number density and respective size strongly depend on the growth temperature and on the flux of germanium atoms [34]. This indicates that the resulting surface morphology is determined by the kinetic parameters of the nucleation and growth processes.

During epitaxy of the stressed layers, the three-dimensional islands begin to grow immediately after their nuclea-

tion by attaching atoms from the supersaturated layer of adatoms, which is usually created by an external atomic flux [57]. Calculations show that stressed layers have a higher equilibrium concentration of adatoms than unstressed layers [60]. The growth of islands due to absorption of the excess adatoms is rapid, even if the external flux of adatoms is blocked. This property of the nucleation process, which requires supersaturation, makes it practically impossible to control the fabrication of very small islands with sizes just slightly bigger than that of the critical nuclei. Moreover, the instability and decay of a fraction of the two-dimensional layer constitute an additional source of atoms for their growth, which may be called self-induced.

In region II of experimental conditions shown in Fig. 5f, the unstable two-dimensional layer favors stimulated nucleation of three-dimensional islands in it. Such nucleation has been achieved by irradiating the sample with a focused electron beam at room temperature. After annealing at 570 °C, each irradiated point exhibited formation of a three-dimensional island [56]. It is a well-known fact that for phase transitions in a bulk the defects and impurities in the supersaturated phase serve as nucleation centers for the new phase. We may assume that in our case the mechanism was similar. Irradiation by an electron beam may create point defects and introduce impurities in the form of carbon atoms. These defects violate the uniformity of the two-dimensional layer and, therefore, serve as growth centers for three-dimensional islands.

In experiments on fabricating three-dimensional nanostructures, STM probes have been utilized to observe the growth of such nanostructures on the surface of a two-dimensional germanium layer on silicon under annealing, with the thickness of germanium layers varying from 2 to 3 BL. These observations also directly indicate that the two-dimensional layer partially decays after emerging three-dimensional structures and represents a source of atoms for their growth [61, 62].

To calculate the minimum size of a three-dimensional island that might be fabricated on a surface with a stable morphology, it was suggested that after nucleation the islands grow only at the expense of germanium atoms produced by the decay of a single bilayer. This amount of germanium ensures the formation of truncated pyramids with a size of about 60 nm at the base and an array density of 6×10^9 cm^{-2}. The formation of such an array of islands is observed in experiments with an incident flux of 0.24 BL min^{-1} at 420 °C (Fig. 1d). These islands are too sizable for spatial quantization effects to manifest themselves in them.

2.5 Instability of two-dimensional germanium layers on other silicon faces

Germanium islands growing on different silicon faces at high temperatures (600 – 700 °C) have been described in Vescan's review [63]. Here, we discuss the stability of the two-dimensional germanium layer in relation to the growth of three-dimensional islands in structures grown at lower temperatures. Instead of the unstable component of a two-dimensional germanium layer on the Si(001) surface, there emerges an intermediate phase of hut clusters, which precedes the formation of equilibrium 'macroscopic' islands [7]. The existence of this intermediate phase was assumed to be the result of competition between growth processes and processes aimed at creating a surface morphology that is in thermodynamic equilibrium. This competition lies in the fact that the hut clusters emerge and grow faster and, hence, appear on the surface earlier than the energy-preferable but slowly growing macroscopic islands. The extremely easy formation of hut clusters explains why the unstable two-dimensional germanium layer has not been observed on the Si(001) surface in many experiments (see Refs [7, 19 – 21, 58, 64, 65]) in which the surface was studied after stopping growth.

A thermally stable two-dimensional germanium layer on Si(001) is 3 ML thick [19, 64]. Nevertheless, the two-dimensional germanium layer may become even thicker when the monitoring of layer thickness is done directly during growth. By measuring the intensity oscillations of the diffraction reflections by the HEED method, Sakamoto et al. [66] and Miki et al. [67] observed two-dimensional growth of germanium on Si(001) to layer thicknesses of about 6 ML, when the growth occurred under relatively high fluxes of germanium atoms incident on the surface. With the help of an ellipsometer, Osipov et al. [68] established that the two-dimensional germanium layer on Si(001) gets thinner after the nucleation of three-dimensional islands. The unstable component of the two-dimensional layer has enough time to decay after island nucleation until the growth process is terminated and the sample cools down to room temperature. Here, the formation of hut clusters is limited not only by the kinetics of surface processes but also by the thermodynamically directed formation of {105} faces, which amounts to these faces becoming longer in energy-preferable directions [69]. The formation of elongated hut clusters is accompanied by the formation of dimples in the two-dimensional layer.

During epitaxy of germanium on other silicon faces, such as Si(113) [33] and Si(105) [32], the thickness of the two-dimensional layer at which the external flux of atoms triggers the formation of three-dimensional islands decreases as the growth temperature rises. Earlier such a temperature dependence was observed by Marée et al. [20] when they constructed the phase diagram of germanium on Si(111); in Ref. [56], we associated this dependence with the existence of an unstable two-dimensional layer (boundary *A* in Fig. 5f). Since the thickness of a thermally stable two-dimensional germanium layer between three-dimensional islands is, probably, temperature-independent, the fact that such a dependence exists indicates that there are unstable two-dimensional germanium layers at low deposition temperatures in the case of Si(113) and Si(105) surfaces, too. Notice that in the course of growth of heteroepitaxial structures of semiconducting III – V compounds, there is a pause of several dozen seconds in deposition after island nucleation and before the III – V compound of another composition begins to grow into these islands [1]. During this pause there is spontaneous island growth and a thermally stable surface morphology is formed. Thus, the partial decay of the two-dimensional layer after nucleation of three-dimensional islands is a general property of growth of various materials in the SK regime [70].

2.6 Effect of atomic steps on island nucleation

The presence of single atomic steps has no effect on the nucleation and growth of three-dimensional germanium islands on Si(111), but the effect of echelons of steps is significant. Echelons of steps are usually created by the process of electrically stimulated surface migration of atoms, which runs in the presence of a constant electric field at high sample temperatures [71]. The germanium deposition on a silicon surface with echelons of steps at relatively low

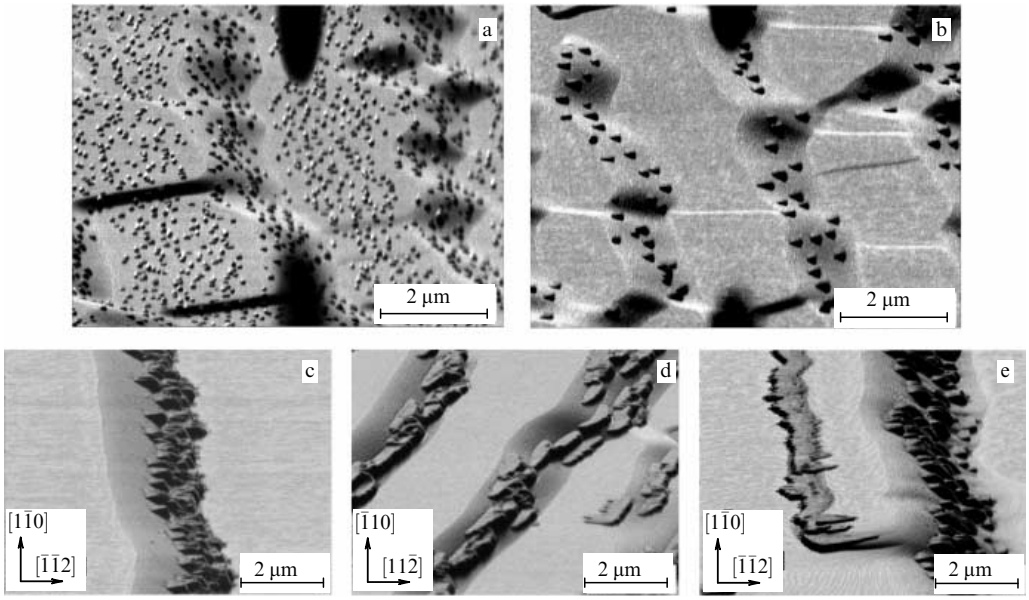

Figure 6. SREM images of silicon surfaces slanted by 2° in relation to the (111) plane in the directions [$\bar{1}\bar{1}$2] (a – c, e) and [11$\bar{2}$] (d) after the deposition of 4.3 BL of germanium at 400 °C (a), 3.6 BL at 500 °C (b), and 13 BL at 650 °C (c – e). The angle of deflection from Si(111) of the sections of the surface with echelons of steps is approximately 6°.

temperatures (400 °C) leads to the formation of high islands both on the terraces of steps and on the surface of echelons of steps. Depletion zones form in the sections along the boundary separating the flat terraces from the echelons of steps, and within these zones the three-dimensional islands do not form (Fig. 6a) [72].

Figure 6b demonstrates that as the temperature rises the size of the depletion zone increases so much that at 500 °C it encompasses the entire terrace. As a result, three-dimensional islands form only on the surface of the echelons of steps, despite the fact that the amount of deposited germanium exceeds 3 BL, i.e., the amount needed for nucleation of three-dimensional islands on Si(111) without the echelons of steps. This process of island formation may be called selective. The result obtained shows, among other things, that the diffusion length of germanium adatoms on Si(111) at 500 °C exceeds half the terrace width, i.e., 1 μm.

Atomic steps on Si(111), whose front directions are along [$\bar{1}\bar{1}$2] and [11$\bar{2}$], differ in the configuration of the atoms at the edge. Figures 6c and 6d illustrate how selective formation of islands happens on the echelons of steps of both types. The common property of the islands was the presence of the facet with the (111) orientation and a 7 × 7 reconstruction at their apices. However, only in the case of steps with their front directed along [11$\bar{2}$] were the islands elongated along the direction of the step edge. The preferable growth of islands along this direction leads to their coalescence along the echelon of steps, as shown in Fig. 6d.

The difference in shape of germanium islands manifested itself most vividly on a surface containing the echelons of steps of both types with the front direction along [$\bar{1}\bar{1}$2] and [11$\bar{2}$]. Such a surface morphology was created by accident as a result of prolonged annealing of the sample, similar to the case described by Latyshev et al. [14, 73]. Figure 6e demonstrates that a solid band of germanium formed along the echelon of steps with the front directed along [11$\bar{2}$], while only separate islands appeared on the surface of the echelon of steps with the front directed along [$\bar{1}\bar{1}$2]. Echelons of steps of both types can be fabricated by photolithography. This possibility makes it possible to implement selective growth of germanium in the form of bands or islands at specified locations on a silicon surface [74]. Sections of the Si(001) and Si(111) surfaces become anisotropic for surface processes after the echelons of steps have formed on them, while the Si(113) surface is completely anisotropic. Germanium deposition on it leads to the formation of germanium nanowires directed along [33$\bar{2}$] [75, 76].

2.7 Formation of germanium islands in Si(111) windows in a silicon oxide layer

The properties of a two-dimensional germanium layer on silicon can be employed for dedicated fabrication of germanium islands at fixed points on the silicon surface. To achieve this, germanium was deposited on an oxidized silicon surface containing windows of pure silicon [77]. The windows were 'opened' by a focused electron beam, and the method relied on the fact that irradiation of silicon oxide by an electron beam lowers its thermal decomposition temperature [78, 79]. Irradiation destroys the chemical bonds in SiO_2, with the result that it decomposes into SiO and oxygen molecules which desorb [80]. Thermal decomposition of the oxide which consists mostly of SiO, happens at temperatures that are about 80 °C lower than the temperature at which SiO_2 decomposes. The method relies on operating with a focused electron beam 2 – 4 nm in diameter that hits the sample, which is subsequently annealed at 720 – 750 °C, and makes it possible to create silicon windows with a minimum size of about 10 nm in an oxide film 0.5 nm thick on a silicon substrate [78, 79]. Windows in a silicon oxide film can also be made by using an STM probe [81].

Silicon windows on an oxidized silicon surface can be seen in SREM images in the form of light dots against a dark background, since the intensity of the electron beam mirror-reflected from the sections of pure silicon surface is much higher than that reflected from the oxide. After germanium is deposited at elevated temperatures of the substrate, the

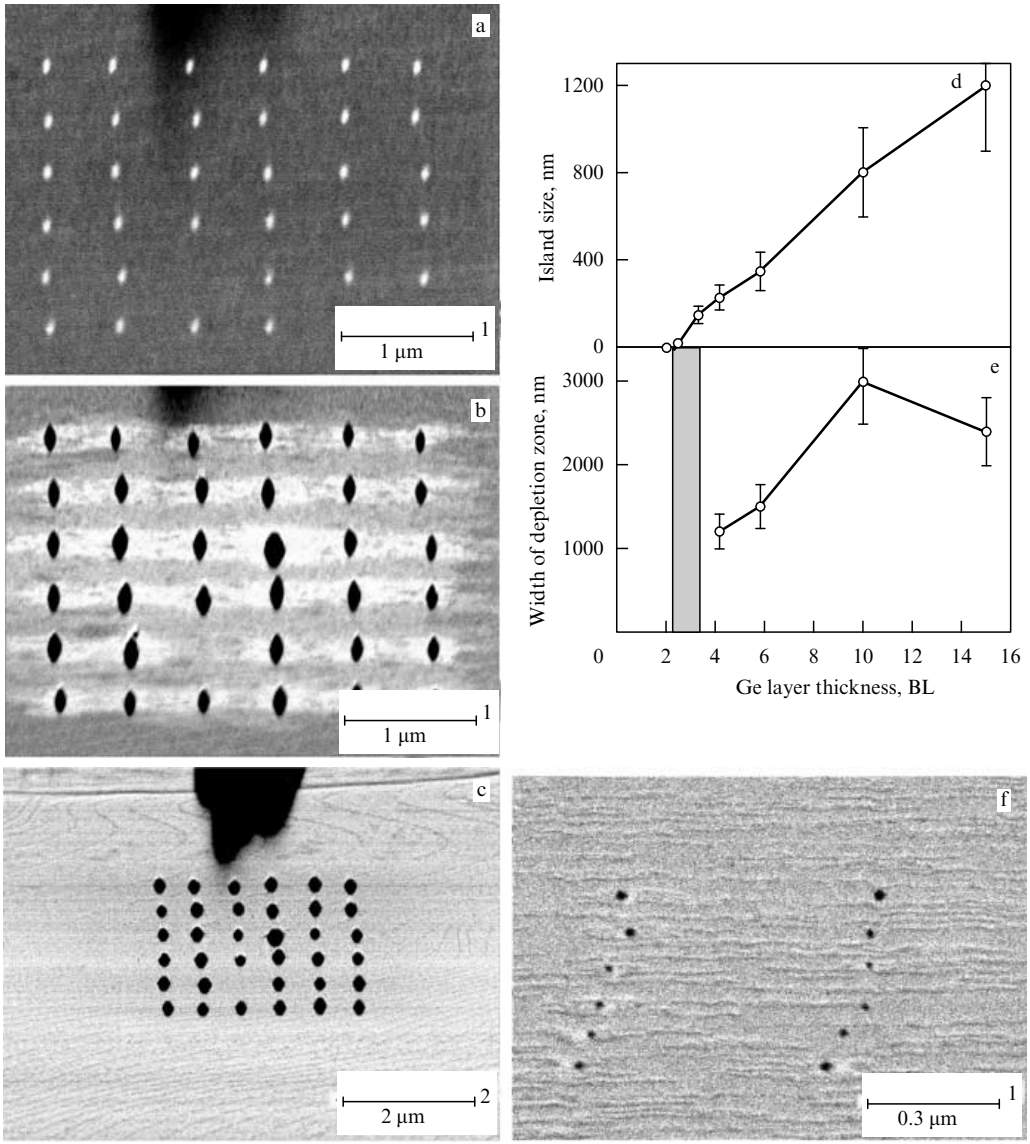

Figure 7. SREM images of a surface at different stages of germanium island formation: (a) a silicon oxide layer with windows of pure Si(111) surface after deposition of 3.3 BL of germanium at 550 °C (the windows appear as light dots), (b) after decomposition of silicon oxide as a result of annealing at 690 °C for 5 min, and (c) after an additional 5-min annealing at 690 °C. The large dark structure in the upper part of the image is the shadow from an SiC particle used as a reference point on the surface. (d) The size of islands formed at silicon window locations in a silicon oxide layer, and (e) the width of the depletion zone around the islands, which is a two-dimensional germanium layer, as a function of the amount of deposited germanium. After germanium deposition there was annealing at 690 °C for 10 min. The hatched stripe in the figure shows the range of coating thicknesses within which islands formed only in windows. (f) SREM image of germanium islands formed at the locations of silicon windows after the deposition of 2.5 BL of germanium at 550 °C and subsequent 10-min annealing at 690 °C. The location of each window was manually fixed by setting the electron beam to bear on the given point at the surface.

difference in contrast between Ge/Si and $Ge/SiO_2/Si$ sections in SREM images becomes more pronounced (Fig. 7a). According to HEED patters, the Ge/Si sections possess a 1×1 structure.

Fujita et al. [79] found that the decomposition temperature of silicon oxide covered with germanium is lower than the decomposition temperature of silicon without germanium. This finding could be due to the formation and desorption of GeO molecules participating in the following reaction

$$SiO_2(surf) + Ge(surf) \rightarrow SiO(gas) + GeO(gas)\,. \qquad (6)$$

Figure 7b presents an SREM image with the black dots corresponding to three-dimensional germanium islands that emerged at the locations where silicon windows appeared after annealing the sample. The 5×5 superstructure, which is typical of germanium layers on Si(111), was observed in HEED patterns from both the light and dark sections in the SREM images of the surface surrounding the islands [77]. The emergence of the 5×5 superstructure indicates that the silicon oxide film has completely decomposed.

SREM images like the one in Fig. 7b show that the sections of the surface around islands appear to be lighter than those far from the islands. Notice that the images of the light sections are elongated by a factor of approximately eight in the horizontal direction, compared to the vertical direction, due to the glancing angle of incidence of the initial electron beam. The distinction in brightness implies that there is a

difference in thickness of germanium layers on Si(111) and shows that the two-dimensional germanium layer around the islands is thinner than it is far from the islands. The sections of thinner germanium layers may have formed at the expense of germanium diffusion to the three-dimensional islands. Figure 7c demonstrates that additional annealing makes the three-dimensional islands bigger and that a homogeneous (in thickness) two-dimensional germanium layer forms on the remaining surface. It should be noted that smaller magnification was used in producing the image in Fig. 7c. This was done with the aim to show that the surface contained no other germanium islands besides those that formed at window locations.

After complete thermal decomposition of the remaining silicon oxide film has been achieved, the surface morphology begins to substantially depend on the germanium coating thickness. At coatings thinner than 2.2 BL, only a two-dimensional layer forms over the entire surface. In the thickness range extending approximately from 2.2 to 3.3 BL, marked by the hatched stripe in Fig. 7e, three-dimensional germanium islands emerge only in windows, with the two-dimensional layer covering the entire remaining surface. At greater coating thicknesses, the surface contains sizable germanium islands that formed over the windows, the depletion zone around the islands (which is the two-dimensional layer), and spontaneously nucleated germanium islands over the remaining part of the surface (Figs 7d and 7e). The difference in thicknesses of the germanium coatings needed for the emergence of spontaneously nucleated islands in the cases of a clean surface and a surface covered with silicon oxide shows that about 1 BL of germanium is spent to completely decompose a 0.5-nm-thick silicon oxide layer, with volatile GeO molecules being produced in the process, and that germanium atoms may diffuse to the silicon surface layer. The size of the islands that formed atop the windows gradually decreases as the germanium coating gets thinner (Fig. 7e). Islands with a base size of about 20 nm were produced when the coating thickness was about 2.5 BL (Fig. 7f).

3. Formation of germanium islands on an oxidized silicon surface

In Section 2 we showed that spontaneous growth of germanium islands immediately after their nucleation on a silicon surface does not allow us to create islands smaller than 10 nm. Fabricating such islands requires modification of the silicon surface. It has been established that preliminary deposition of such elements as antimony [82, 83] or carbon [84–86] in an amount up to a single monolayer stimulates the nucleation of three-dimensional islands upon subsequent germanium deposition. In the case of antimony, the island number density reaches 5×10^{11} cm^{-2} [83]. A temporarily coating of the silicon surface with a xenon layer also creates the necessary conditions for the nucleation of germanium islands [87, 88]. Germanium forms a layer of islands if its deposition is made on a nitrided silicon surface [89]. However, the best result is achieved when germanium is deposited on an oxidized silicon surface with the oxide's thickness in the 0.3–0.5-nm range [11, 90–94]. In this case, the germanium islands form with an ultimately high number density of about 2×10^{12} cm^{-2} and have a hemispherical shape. Barski et al. [95] studied the possibility of using even thicker silicon oxide layers. Below, we shall examine the mechanism of germanium island growth on an oxidized silicon surface.

3.1 Size and structure of islands

One of the key features of germanium island formation on an oxidized silicon surface is the nucleation of three-dimensional islands immediately after the onset of deposition, i.e., the process does not include the formation of a two-dimensional wetting layer [11]. Figure 8 demonstrates that deposition of 2.6 BL of germanium at 430 °C leads to the formation of dome-shaped islands with a base diameter of 7.5 ± 1.5 nm and a height of about 2.5 nm. The density of the island array in the layer may be as high as 2×10^{12} cm^{-2}. At much higher growth temperatures (such as 670 °C), the island array density rises by a factor of approximately 1.4 and the base size of the islands drops to 5.5×2.0 nm. The size distribution of the islands exhibits a single peak and shows a total absence of islands with sizes that differ substantially from the average size. Notice that the real diameter of the islands may be somewhat smaller than the size determined from STM images. The reason is the effect of the shape of the tip of the STM probe on the image of an island's base when the base does not gradually slope, as in our case of hemispherical islands. Also note that at a number density of 2×10^{12} cm^{-2}, the average distance between islands amounts to about 7 nm. Such density may be considered ultimately high for islands down to 10 nm at the base.

Despite the fact that germanium is deposited on the amorphous surface of silicon oxide, the HEED patterns demonstrate that under certain growth conditions, depending on the substrate temperature and the germanium deposition rate, germanium islands grow epitaxially in relation to the crystalline silicon substrate. The presence of Debye rings in the HEED patterns (Fig. 9a) indicates that the germanium islands were crystalline, but they were oriented randomly with respect to the substrate at low growth temperatures. The appearance of point reflections in the HEED patterns (Fig. 9b) is evidence of diffraction arising from the scattering of electrons by the three-dimensional islands grown epitaxially at 500 °C.

These data are supported by the results obtained with high-resolution TEM, which show that the islands are crystalline and dome-shaped (Figs 9d–f). The crystalline islands grown at low temperatures are oriented at random in relation to the crystal lattice of the substrate and are separated from it by a thin layer of silicon oxide (Figs 9d, e). At high temperatures, the islands grow epitaxially (Fig. 9f). The data obtained by different groups of researchers [11, 90–96] are in good agreement. Yakimov et al. [91] obtained a TEM image of germanium islands in the surface plane, which supports the STM data on the domelike shape of the islands and their high number density.

3.2 Causes of epitaxial growth

Epitaxial growth of germanium requires that there be the sections of a clean silicon surface. Such sections appear as a result of the interaction between adatoms of the germanium being deposited and silicon oxide according to the reaction

$$\mathrm{SiO_2(surf)} + \mathrm{Ge(adatom)} \rightarrow \mathrm{SiO(gas)} + \mathrm{GeO(gas)}\,. \quad (7)$$

At elevated temperatures, the SiO and GeO molecules are the volatile reaction products. With the aid of reflection electron microscopy, Shimizu et al. [97] and Kosolobov et al. [98]

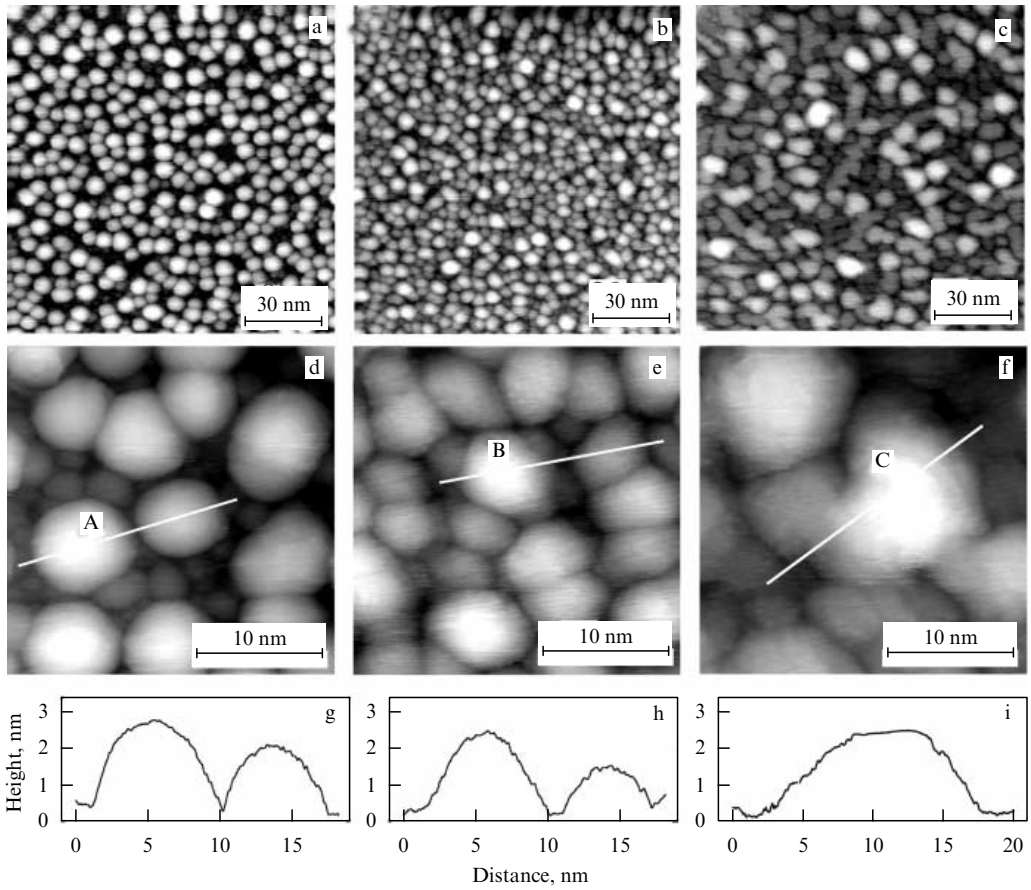

Figure 8. STM data on germanium islands formed after depositing 2.6 BL of germanium at a rate of 0.5 BL min^{-1} on the oxidized Si(111) surface at 430 °C (a, d, g), 670 °C (b, e, h), and 740 °C (c, f, i). The data contain the height profiles along the white lines labelled *A* for profile (g), *B* for profile (h), and *C* for profile (i).

found that when oxygen molecules interact with a clean silicon surface, gas etching of the silicon accompanied by formation of volatile SiO molecules occurs already at such low temperatures as 500 °C. Such a temperature for desorption of SiO molecules agrees with the results of kinetic studies of this reaction [99]. The evaporation of GeO molecules as a result of the interaction of oxygen molecules with a clean germanium surface has been recorded at even lower temperatures, such as 360 °C [100]. According to reaction (7), one can expect the formation of volatile products at temperatures that are lower than those at which oxygen molecules interact with clean silicon surfaces, due to the lower desorption temperature of GeO molecules. In our experiments running at a rate of 0.5 BL min^{-1} of germanium deposition on an oxidized silicon surface, the emergence of epitaxial germanium islands was observed at as a low temperature as 430 °C, which may be called the lower temperature limit of epitaxial growth [11].

The upper temperature limit for the formation of three-dimensional epitaxial germanium islands on an oxidized silicon surface has also been established. STM images (see Fig. 8) demonstrated that the islands coalesce and flatten out at growth temperatures above 670 °C. Such change in shape agrees with the relevant change in the HEED pattern shown in Fig. 9c. At such high temperatures, a substantial fraction of silicon oxide is desorbed at the initial period of germanium deposition, with the result that the growth conditions become similar to the conditions of germanium heteroepitaxy on a clean silicon surface.

The temperature range of epitaxial growth of germanium islands depends on the germanium deposition rate. HEED patterns have shown that the islands grown at a deposition rate of 0.05 BL min^{-1} at 430 °C are epitaxial, while the islands are oriented at random in relation to the silicon substrate at a deposition rate of 2.0 BL min^{-1}. Since at a lower deposition rate the sample was exposed to the growth temperature for a longer time, it might be assumed that during this time the reaction proceeds at the boundary between the germanium island and silicon oxide that leads to epitaxial formation of the island. If the role of the reaction at the island – Ge/SiO_2 boundary were significant, prolonged annealings of the nonepitaxial germanium islands would transform them into epitaxial. However, experiments have revealed that annealing does not transform nonepitaxial islands into epitaxial [11]. From these experiments it follows that the conditions necessary for epitaxial growth are created as a result of the reaction (7) between germanium adatoms and the oxidized silicon surface in the initial stage of germanium deposition, i.e., before island nucleation has taken place. STM images have also shown that the shape of both epitaxial and nonepitaxial islands does not change as a result of subsequent annealings for 30 min at the growth temperatures, which indicates that the islands are thermally stable.

3.3 Nucleation mechanism

To determine the mechanism of island nucleation, the number density of the islands has been measured as a function of such

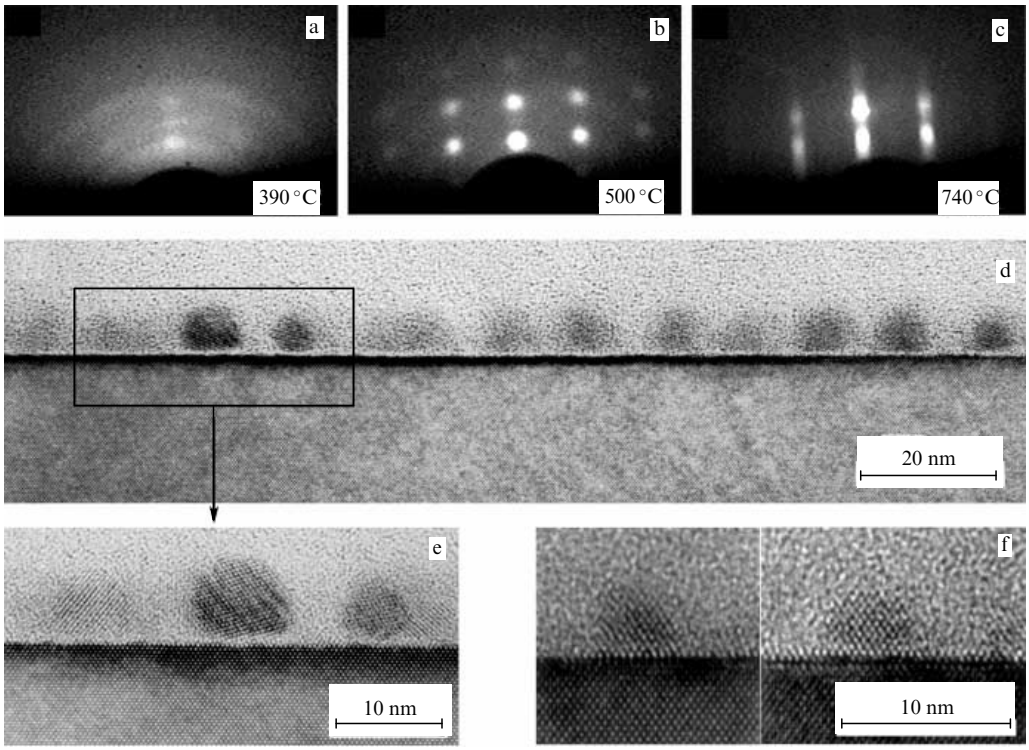

Figure 9. (a – c) HEED patters of germanium islands grown under deposition of 2.6 BL of germanium on an oxidized Si(111) surface at temperatures indicated in the images. The germanium deposition rate was 0.5 BL min^{-1}. (d – f) Images of germanium islands according to TEM data. The islands were grown under deposition of 12 ML (d, e) and 8 ML (f) of germanium on an oxidized Si(001) surface. The substrate temperature was 390 °C (d, e) and 450 °C (f).

parameters as growth temperature, deposition rate, and coating thickness. Islands become clearly distinguishable in STM images after one or more germanium bilayers has been deposited (Fig. 10). Figures 10a – f indicate that within the range of coating thicknesses extending from 1 to 7 BL the island array density does not change and is approximately equal to 2×10^{12} cm^{-2} for oxidized surfaces, either Si(111) or Si(001) [101]. The very fact that the island array density remains constant is important from the practical angle, since it means that the island size is determined solely by the amount of deposited germanium.

Figure 10g gives evidence that the island array density is practically growth temperature-independent from 330 °C to 620 °C and is the same for oxidized Si(111) and Si(001) surfaces. It is also identical for epitaxial and nonepitaxial islands. This points to the fact that the surface reactions determining the nucleation mechanism are similar for the entire temperature range under investigation.

Direct information about the nucleation mechanism is contained in the dependence of the island array density on the flow rate of the germanium atoms falling onto the sample's surface. The experimental data suggest that this density remains constant for atomic fluxes ranging from 0.05 to 4 BL min^{-1} (Fig. 10g). Since the deposition rate specifies the adatom concentration on the surface, this result means that the probability of an island nucleus forming is independent of the adatom concentration.

The independence of the island array density from the growth conditions is possible when the initial surface contains a fixed number of structural 'defects' that serve as growth centers for islands. Various methods have been employed in the investigation of the oxidized silicon surface, and no special features of the structure of the surface that would have a concentration of 10^{12} cm^{-2} were discovered. At the same time, it is known that metals deposited on an SiO_2 surface also form island arrays with a density of order 10^{12} cm^{-2} [102]. Here, the array density depends on the kind of metal and for some metals differs in magnitude by a factor of almost ten. Another process that characterizes the state of an oxidized silicon surface amounts to the surface thermal decomposition according to the reaction $SiO_2 + Si \rightarrow 2SiO$. This process also involves nucleation, but the nuclei are pores. Their number density varies between 10^9 and 10^{10} cm^{-2} [103, 104], which is much lower than the germanium island array density. In the next section we shall show that the growth of silicon on an oxidized silicon surface also occurs via nucleation of three-dimensional islands, but with a number density amounting to 10^{13} cm^{-2} [17]. All these facts give evidence that the density of an island array on an oxidized silicon surface is not related to a definite type of structural features; rather, it is determined by the reaction parameters characterizing the interaction between the surface and the deposited atoms.

The independence of the density of a germanium island array from the adatom concentration is possible if a single adatom becomes, as a result of its reaction with the surface, a nucleus capable of further growth. According to the theory [see Eqn (2)], the density N of an island array is proportional to the flow rate F of the atoms according to the law $N \sim F^p$, where the exponent p is a function of the critical nucleus size i [105, 106]. In our case, p is nearly zero (Fig. 10h), with the result that i is zero, too. If by the stage of nucleation of islands we mean a process that switches on the interaction between adatoms, then $i = 0$ corresponds to a situation in

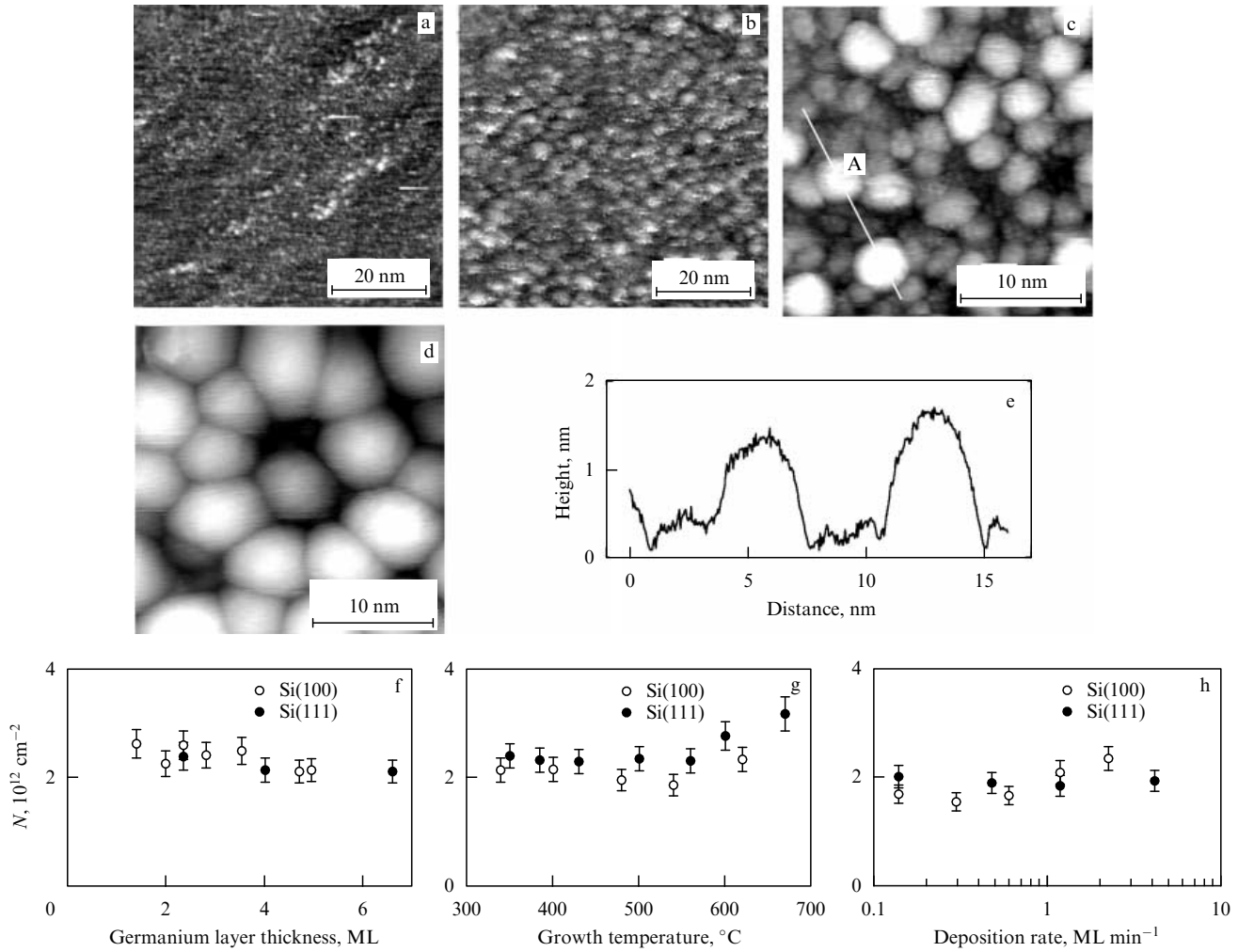

Figure 10. STM images of surfaces obtained before (a) and after (c and d) germanium deposition at a rate of 0.5 BL min^{-1} at 600 °C on an oxidized Si(111) surface. The amount of deposited germanium was 0.5 BL (b), 1.0 BL (c), and 2.6 BL (d). (e) The height profile measured along the white line *A* in Fig. 10c. The dependence of the island number density on (f) the amount of germanium deposited at a rate of 0.5 BL min^{-1} on oxidized Si(001) (growth temperature 400 °C) and Si(111) (growth temperature 430 °C) surfaces, (g) the growth temperature as 2 BL of germanium is deposited at a rate of 0.5 BL min^{-1}, and (h) the germanium deposition rate for 2 and 2.6 BL coating thicknesses at growth temperatures 480 and 430 °C on Si(001) and Si(111), respectively.

which the growth of islands begins without this stage as a result of the interaction between a single adatom and the surface.

The mechanism of nucleation at low growth temperatures when a single germanium adatom reacts with the silicon oxide surface probably consists in the rupture of the Si–O bond. The same process takes place when volatile SiO and GeO molecules are formed by reaction (7) at higher temperatures. This process guarantees the formation of surface sections of pure silicon needed for epitaxial growth. The fact that array densities of epitaxial and nonepitaxial germanium islands are the same is an indication that this reaction limits nucleation in both cases.

3.4 Density estimates

We derive an equation for the density of an array of islands in their nucleation via the reaction between one adatom and the surface. The diffusion length x of germanium adatoms on a silicon oxide surface defines the distance d between islands: $d = 2x$. The diffusion length is given by the formula

$$x = (D\tau_r)^{1/2}, \tag{8}$$

where $D = va^2 \exp(-E_d/kT)$ is the surface diffusion coefficient of the adatoms, v is the frequency of their oscillations ($v \approx 10^{13}$ s^{-1}), a is the adatom hopping distance, E_d is the diffusion activation energy, and τ_r is the adatom lifetime on the surface. At the initial instant of germanium deposition on the surface, when nuclei of islands begin to form, the adatom lifetime is determined by the nucleation reaction and is described by the formula

$$\tau_r^{-1} = k_r^{(0)} \exp\left(-\frac{E_r}{kT}\right), \tag{9}$$

where $k_r^{(0)}$ is the pre-exponential factor of the reaction rate constant, and E_r is the reaction activation energy. Since the island array density $N = d^{-2}$, combining formulas (8) and (9) we get

$$N = \frac{k_r^{(0)}}{4va^2} \exp\left(\frac{E_d - E_r}{kT}\right). \tag{10}$$

The fact that the island array density is temperature-independent implies that $E_d \approx E_r$. The adatom hopping

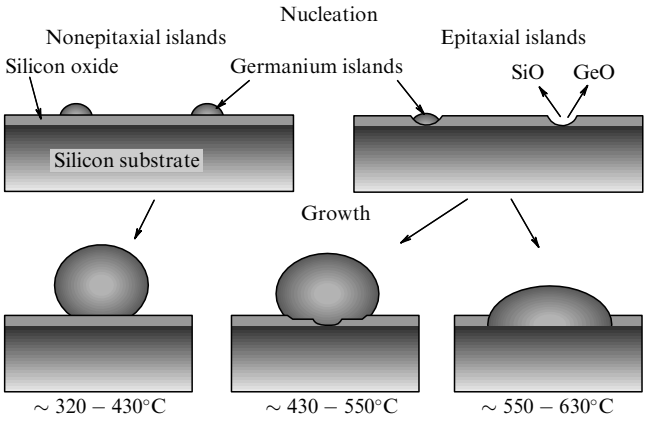

Figure 11. Schematic of the formation of germanium islands on an oxidized silicon surface at different temperatures.

distance a is determined by the repetition period of the surface structure, so that $a \approx 0.3$ nm on silicon oxide. For surface reactions, the factor $k_r^{(0)}$ is not simply the adatom oscillation frequency, i.e., not every adatom oscillation results in a reaction. For reactions between an adatom and the surface atoms, the ratio $k_r^{(0)}/\nu$ usually varies between 10^{-2} and 10^{-3} [107]. Then Eqn (10) yields the estimate $N \sim 10^{12}$ cm^{-2}, which coincides in order of magnitude with the density of the array of germanium islands that form on the oxidized silicon surface. Since $N = d^{-2} = x^{-2}/4$, the diffusion length of the germanium adatoms on the oxidized silicon surface is about 4 nm.

It should be noted that different researchers have obtained expressions similar to Eqn (10) for conditions where the concentration of adatoms on the surface was determined by the balance between deposition and rapid desorption [108, 109]. What makes our case so specific is that deposition takes place in conditions of complete condensation, and a stable nucleus is formed when a single adatom interacts with the surface.

The size of the section of pure silicon surface needed for epitaxial growth of germanium islands is determined by the relation between the surface reaction rates. The experimental data suggest that the size of this section is smaller than the area of an island base at growth temperatures of up to 600 °C. This means that the rate of decomposition of the silicon oxide by reaction (7) is much lower than the rate of attachment of germanium adatoms to the nucleated island. As a result of such a rate ratio, the silicon oxide decomposition occurs before the nucleation of islands, while after their nucleation they become centers of attachment of germanium adatoms. This leads to island growth above the surrounded sections of silicon oxide (Fig. 11). The respective structure is less stressed than the structure of germanium islands on silicon, which are grown on a pure silicon surface in the SK regime. This evidence agrees with the results of theoretical calculations, which show that the stress energy decreases as the islands become spherical. With such islands the contact with the substrate is at its minimum and characterized by minimum possible stress.

As the temperature increases, the rate of silicon oxide decomposition rises faster than the rates of surface diffusion and incorporation of adatoms into a growing island. This happens because of the higher activation energy of oxide decomposition, amounting to about 3 eV, which is much larger than 1 eV corresponding to the energies of diffusion activation and incorporation of adatoms into an island. As a result, the size of the area of direct contact between island atoms (germanium) and the substrate (silicon) increases and the island flattens out.

3.5 Local structure

The structure of germanium islands has been studied by Kolobov et al. [90, 110, 111] who relied on the method of extended X-ray absorption fine structure after the sample was exposed to air [90, 110, 111]. The spectra of nonepitaxial islands grown at 380 °C are identical to the germanium spectrum in the bulk, i.e., they do not carry any traces of germanium oxide phases and, hence, are stable with respect to oxidation at room temperature. At the same time, the spectra of epitaxial islands grown at 450 °C may be represented by a superposition of the spectra of metallic germanium and GeO_2. The results of fitting have shown that the fraction of the oxidized phase amounts to about 50%. Wei et al. [112] also attempted to fit the spectrum of epitaxial islands to the spectrum expected from the Ge–Si alloy. The spectrum from the alloy was found to differ significantly from the measured one. This makes it possible to conclude that the mixing of germanium and silicon atoms is negligible in the case of epitaxial islands.

There are two factors that determine the difference between epitaxial and nonepitaxial germanium islands from the viewpoint of the reactivity of their surfaces. Epitaxial islands possess a crystal structure experiencing elastic strain caused by the silicon substrate, which also affects the reconstruction of the island surface. As is known, germanium is more inert to oxidation at room temperature, compared to silicon: the sticking coefficient of O_2 molecules to the Ge(111) surface is smaller by a factor of 100 than that of O_2 molecules to the Si(111) surface. Furthermore, the O_2 adsorption on germanium becomes saturated already at such a thin coating as 0.1 ML, which shows that only 'defects' (e.g., steps) may serve as locations of adsorption [100]. Hence, being more weakly bonded to the substrate, nonepitaxial germanium islands may have an energy-preferable surface reconstruction, which is devoid of states that are active for the reaction with oxygen at relatively low temperatures. The second factor is that the higher strain of epitaxial islands facilitates oxidation, since oxidation leads to relaxation of stresses.

A characteristic feature of germanium islands in the silicon matrix, which were grown in the SK regime, is the strong mixing of germanium and silicon atoms [110, 113–117] that is favorable for reducing the elastic strains. Although the intensity of the peaks in the Raman scattering spectra is not proportional to the number of the respective atomic bonds in structure [118], the very weak intensity of the peak in Raman scattering associated with the vibration of Si–Ge bonds is an indication that the mixing of atoms in structures grown with the use of oxidation of the silicon surface is insignificant [119]. The characteristic of the state of germanium islands in the silicon matrix is contained in the position of the peak associated with vibrations of Ge–Ge bonds, which is largely determined by two factors, namely, the extent of elastic strain accompanied by the mixing of germanium and silicon atoms, and spatial quantization, which cause, respectively, high- and low-frequency shifts of this peak. The peak is observed at 315 cm^{-1} for structures grown in the SK regime, while for bulky silicon this peak

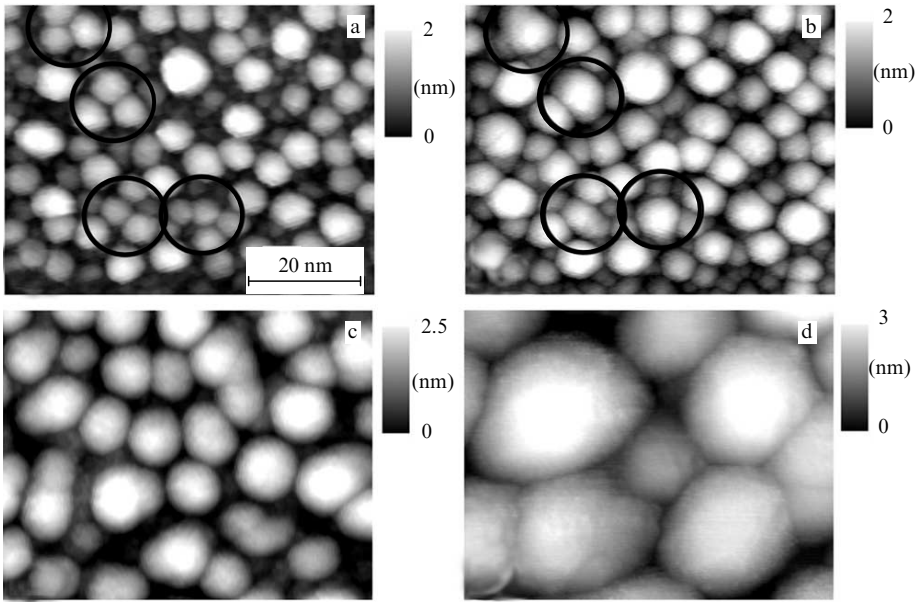

Figure 12. STM images of a surface after the deposition (a) of 2 BL of germanium on the oxidized Si(111) substrate, and subsequent deposition (b, c, and d) of silicon layers with thicknesses equal to 0.3, 1.0 , and 3.0 nm, respectively, on the layer of germanium islands depicted in Fig. 12a. The images (a) and (b) show the same section of the surface. Here, black circles mark the germanium islands that have merged as a result of the silicon growth on them. The selective growth of silicon only on germanium islands can be seen in Figs 12b and c. Germanium and silicon were deposited at 420 °C. All images show the surface sections of the same size.

resides at 300 cm^{-1}. What the shift in the peak's position indicates is that the effect of elastic strain of Ge – Ge bonds is predominant, while the low-frequency shift in the peak's position to 297 cm^{-1}, observed for structures grown at 600 °C with silicon-surface oxidation, reveals that the spatial quantization effect is predominant and, respectively, that the strain on the bonds is weak and the mixing of germanium and silicon atoms is insignificant [114].

The use of a thinner layer of silicon oxide (1 ML thick or even less) fabricated at 400 °C and at relatively high temperatures (550 °C and higher) for germanium growth can lead to substantial mixing of the first germanium layers with the silicon atoms from the substrate. Fonseca et al. [120] observed the formation of germanium islands for this case by recording scattered helium ion beams only after a coating thickness of 0.9 nm was achieved.

3.6 Multilayer structures of germanium islands in the silicon matrix

Fabricating multilayer structures includes the growth of silicon on a layer of germanium islands which, in turn, were grown on an oxidized silicon surface. In the initial stage of this growth, silicon adatoms were selectively incorporated only into germanium islands and do not attach themselves to the surface of silicon oxide between the islands. This becomes obvious if one compares Figs 12a and b. Such a behavior of silicon atoms leads to a continuing growth of three-dimensional islands with germanium islands at their base and does not alter their shape. Coalescence of islands under subsequent silicon deposition creates a 'bumpy' surface morphology (Figs 12c and d) [101]. It should be noted that the silicon growth on a layer of germanium islands formed in the SK regime actually develops by an essentially different mechanism. The deposited silicon 'prefers' to fit into the sections of the surface between the islands [121 – 123]. Since these structures experience a stronger elastic strain, silicon growth is accompanied here by a mixing of germanium and silicon atoms, and by a change in shape of the islands with a tendency of becoming flatter and smaller in size [124].

The density of the germanium island array in the second layer formed on the oxidized surface of the deposited silicon layer was found to be approximately 3×10^{12} cm^{-2}, which is higher by a factor of 1.5 than the density of the island array on the initial flat surface of the substrate (Fig. 13). Since the island number density is determined by the diffusion length of germanium adatoms on the silicon oxide surface, the observed increase in density is the result of both an increase in the effective size of the surface caused by a change in the surface morphology and by a decrease in the diffusion length of the adatoms, caused by the appearance of atomic roughnesses on the surface. HEED patterns revealed that the silicon layer is epitaxial in relation to the substrate in the event of its growth on the epitaxial germanium islands (Fig. 13d) [101]. However, by the very nature of its formation, this layer may carry crystal defects along the boundaries of coalescing silicon islands. The buildup of crystal defects in silicon layers manifests itself in structures containing several layers of germanium and silicon islands in the form of a light background, point reflections from stacking faults, and Debye rings in HEED patterns (Figs 13e and f). A silicon layer that has formed on a layer of nonepitaxial germanium islands possesses a structure consisting of randomly oriented microcrystals.

4. Growth of silicon on an oxidized silicon surface

Growth of silicon on pure silicon surfaces occurs as a result of the movement of atomic steps [12, 13]. Such layer-by-layer growth is used, in particular, in creating quantum wells in a silicon matrix by forming δ-doped layers [15]. Three-dimen-

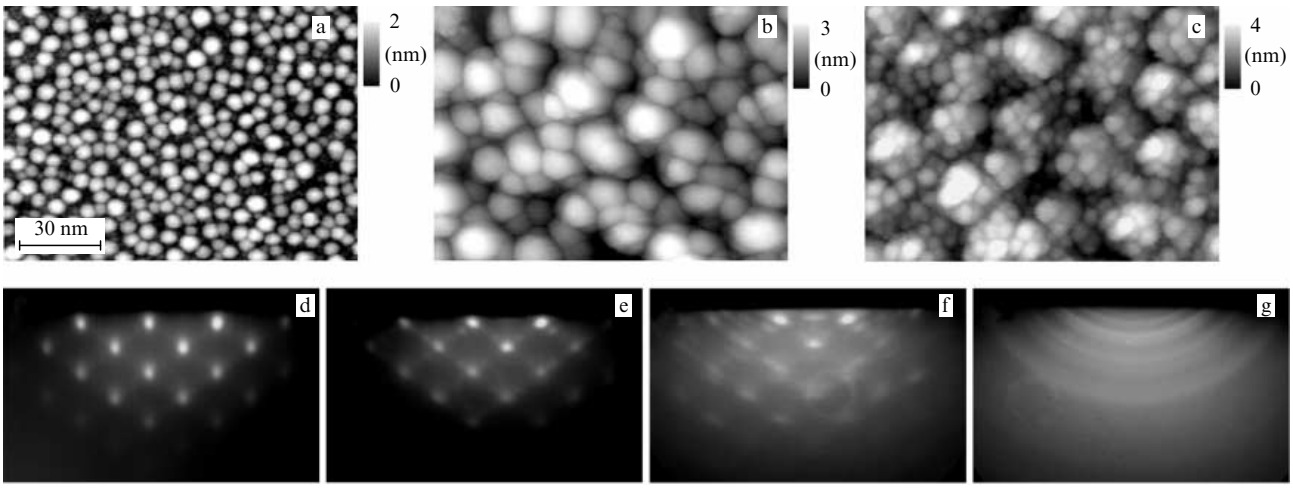

Figure 13. STM images showing evolution of a surface after the deposition (a) of 2 BL of germanium on the oxidized Si(111) substrate, (b) of a layer of 3-nm-thick silicon on a layer of germanium islands, and (c) of 2 BL of germanium on the oxidized surface of the deposited silicon layer. The oxidation of the silicon surface and the depositions of germanium and silicon were carried out at 400 °C. All images depict the surface sections of the same size. HEED patterns were taken from the surfaces of the first (d), third (e), and sixth (f and g) monolayers of 5-nm-thick silicon layer grown at 560 °C (d, e, and f) and 380 °C (g) on layers of germanium islands on an oxidized silicon surface. The nominal thickness of each germanium layer in this case amounted to 3.5 BL.

sional nanoislands of silicon on a silicon surface constitutes a new structure which, possibly, exhibits exciting optical properties. It may be used, as a base, for fabricating structures consisting of quantum dots of doped silicon in a silicon matrix, which potentially have stronger quantum effects than δ-doped layers. The fabrication of three-dimensional silicon nanoislands on a silicon surface is possible by employing an oxidized silicon surface. Here, we discuss the mechanism of this process.

4.1 Morphology and structure of a thin silicon layer

As in the case of germanium growth, the oxidation of silicon surface dramatically alters the conditions needed for further silicon growth. The silicon being deposited forms three-dimensional islands. Here, the shape and structure of the islands depend on the growth temperature. At temperatures between 400 and 570 °C the islands are shaped roughly like hemispheres (Figs 14a, d) [17, 125]. At higher temperatures (from 570 to 640 °C), the islands acquire the form of tetrahedral pyramids.

HEED patterns taken from a surface on which silicon was deposited at about 450 °C contain point reflections against a light background (Figs 14g – j). The location of the reflections suggests that electron diffraction occurs on three-dimensional islands grown epitaxially in relation to the Si(001) substrate. The intensity of the reflections weakens, while that of the background increases as the growth temperature drops to 400 °C. This is an indication that the number of epitaxial islands is decreasing. At 400 °C or below, practically all islands grow nonepitaxially. It should be noted that for germanium [11] the temperature range where epitaxial growth is replaced by nonepitaxial is much narrower than it is for silicon [17]. Saranin et al. [126] revealed that the thickness of silicon oxide layer has no marked effect on the formation of silicon islands at growth temperatures below 450 °C.

Despite the differences in shape and structure, island arrays were found to have a number density that is practically independent of the growth temperature in the range from 400 to 590 °C (Fig. 14k). Many such islands were in contact with each other because of their high number density. Their number was counted on the basis of the following criterion: islands were assumed to be separated if the distance between them was more than half their height. This seems to be a natural criterion if one allows for the fact that the real distance between them may be somewhat larger than the value following from STM data. The smaller distance effect shows itself because of the influence that the size of the STM probe tip has on the image of the edge of three-dimensional islands, which is especially true for hemispherical islands.

4.2 Surface processes in island formation

Nonepitaxial islands grown at 400 °C were found not to become epitaxial after subsequent annealing at 500 °C for 10 min. This property of silicon islands indicates that the reaction between the deposited silicon and silicon oxide does not take place at the boundary between them and that the conditions needed for epitaxial growth are established in the initial deposition stage before germanium adatoms are incorporated into an island. Thus, the sections of pure silicon required for epitaxial growth to occur may appear on the oxidized surface as a result of the reaction

$$\mathrm{SiO_2(surf)} + \mathrm{Si(adatom)} \rightarrow 2\mathrm{SiO(gas)}\,. \qquad (11)$$

It is known that in the case of oxygen adsorption on a clean silicon surface the formation and desorption of SiO molecules proceed at 500 °C or higher temperatures [97, 98] according to the reaction

$$2\mathrm{Si(surf)} + \mathrm{O_2(adsorb)} \rightarrow 2\mathrm{SiO(gas)}\,. \qquad (12)$$

Since epitaxial formation of islands on an oxidized silicon surface is observed at such low temperatures as 420 – 460 °C, we can conclude that the SiO desorption by reaction (11) occurs at lower temperatures than it does by reaction (12). The desorption of submonolayer coatings of silicon oxide via the formation of volatile SiO molecules proceeds with an activation energy of about 3 eV [127 – 129].

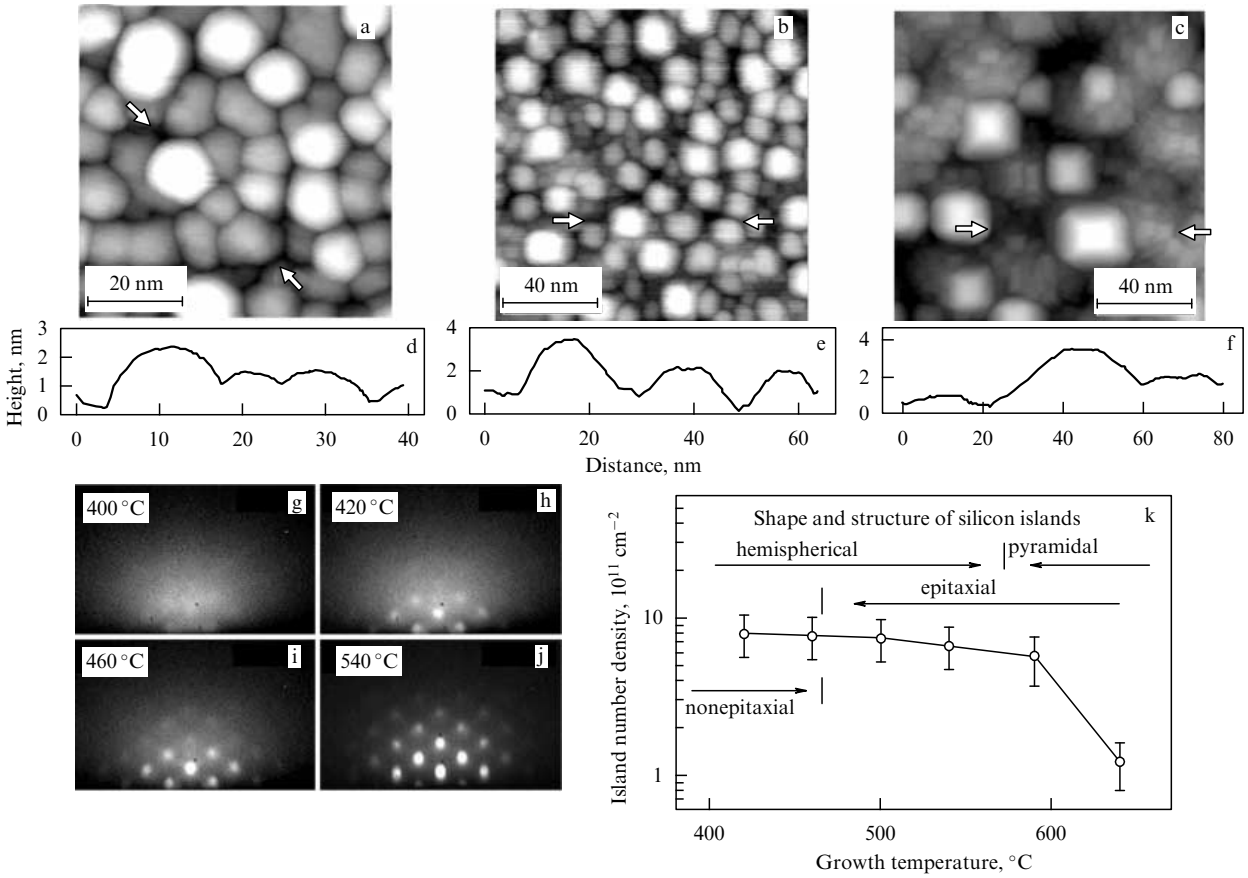

Figure 14. STM images of surfaces that formed after deposition of 5.8 ML of silicon at 420 °C (a), 590 °C (b), and 640 °C (c) on the oxidized Si(001) surface. (d, e, and f) Height profiles measured between the points marked by arrows in Figs 14a, b, and c, respectively. The facets on the lateral sides of the islands have the preferable orientations {113} and {115}. (g, h, i, and j) HEED patterns from surfaces that formed after deposition of 5.8 ML of silicon on the oxidized Si(001) surface at temperatures indicated in the respective images. (k) The temperature dependence of the island number density according to STM data.

The islands may turn hemispherical when the bonds between the atoms in an island are stronger than those between the island atoms and the substrate atoms. Nevertheless, the hemispherical shape observed in the temperature interval extending from 460 to 570 °C is atypical for epitaxial islands. The formation of hemispherical epitaxial islands is a reflection of the competition between reaction (11) and the addition reaction between silicon adatoms and growing islands. After the formation of sections of pure silicon [by reaction (11)] and the nucleation of islands, silicon adatoms are capable of attaching themselves to islands. The activation energy of silicon adatom attachment to an island is low, and the temperature dependence of this process is, on the whole, determined by the activation energy of adatom diffusion to the area where the reaction proceeds, whose magnitude is about 1 eV. At low temperatures, the addition process dominates over reaction (11), and the silicon islands grow in the lateral direction atop the remainder of the silicon oxide layer, as in the case of germanium island growth. Hence, the epitaxial origin of hemispherical silicon islands is determined by the epitaxial nature of their nucleation in the initial stage of silicon deposition. This mechanism creates epitaxial islands that are coupled to the silicon substrate only in the areas of island nucleation, while silicon atoms at the island edges bind to the remainder of the silicon oxide layer. This fact largely defines the hemispherical shape of the islands.

Because of higher activation energy, the rate of reaction (11) increases with a rise in temperature much faster than the rate of adatom attachment to an island. At growth temperatures of 570 °C and higher, reaction (11) ensures the formation of the sections of pure silicon on the substrate surrounding the growing islands, which acquire the shape of tetrahedral pyramids with {311} and {511} facets. Above 570 °C, as the rate of silicon oxide decomposition increases, the spatial density of the islands decreases, with the result that the average island size increases so that some islands grow to 30 nm at their base and exhibit well-developed facets on the lateral faces (Figs 14c, f). Moreover, STM images taken after crystal growth at high temperatures show the presence of (001) terraces and atomic steps between pyramidal islands and the absence of any remainder of the silicon oxide layer. Figure 15 schematically displays the structures for five temperature intervals. The data from LEED patterns and those of characteristic loss spectroscopy of low-energy electrons were also used in determining these structures [125].

At high temperatures, the decomposition of the remaining silicon oxide film continues even after the nucleation of three-dimensional islands. This decomposition creates new sections of a clean silicon surface, which attach the silicon atoms being deposited. The process leads to the formation of small terraces and sections with irregular atomic steps comprising numerous breaks (Fig. 15c).

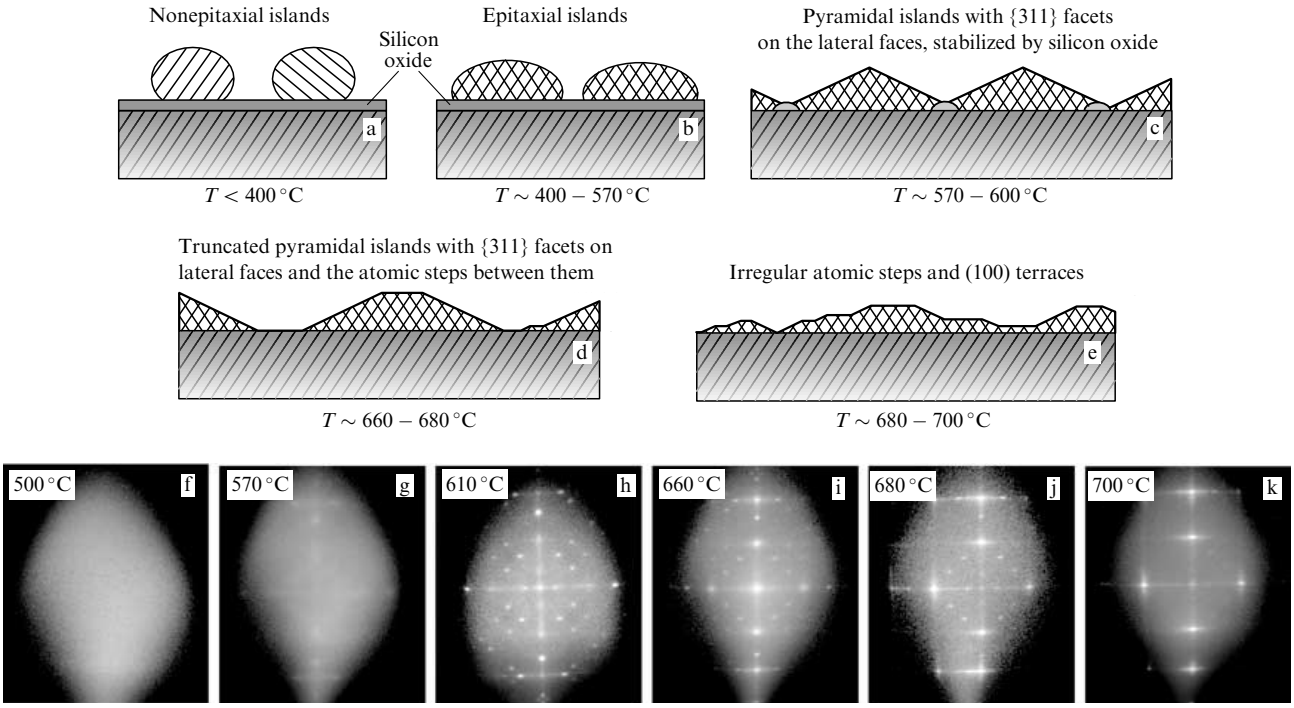

Figure 15. (a – e) Schematics of surface morphology with silicon islands grown on an oxidized Si(001) surface at different temperatures. (f – k) LEED patterns obtained after deposition of 6 ML of silicon on the oxidized Si(001) surface at different temperatures and an electron energy of 52.3 eV. The patterns correspond to the surface morphology shown in Figs 15a – e with point reflections from tetrahedral pyramids with {113} facets on lateral faces and a 3×1 reconstruction. The patterns display the appearance of (100) terraces at high growth temperatures.

The formation of tetrahedral pyramids is a natural process on surfaces with the (001) orientation. For instance, what is known as hut clusters with the facet orientation {015} on the lateral faces are formed as a result of heteroepitaxy of germanium on Si(001) at moderate substrate temperatures [7]. The morphology of pure silicon surfaces oriented at small angles to (001) is created by the stable faces $\{1, 1, 2n + 1\}$, where $n = 1, 2$, etc. [130 – 132]. Facets with such orientations have also been observed on the lateral faces of silicon pyramids grown by gas-phase deposition [133] and ultra-high-vacuum thermal decomposition of disilane in Si(001) windows on an SiO_2 film [134]. The slope of the lateral faces of the islands that form in the windows increased as the islands grew, which corresponds to a gradual transition from the {1, 1, 13} facets to {113} facets through intermediate facets of the above-noted series [134].

The island nucleation and growth mechanism explains why gas-phase chemical deposition on an oxidized silicon surface combined with the use of silanes does not lead to formation of nanostructures with a size of about 10 nm. The formation of volatile SiO molecules, which is needed in order to establish the conditions necessary for epitaxial growth, does not happen in the reaction involving silanes and silicon oxide as long as the temperature is below 600 °C. Silanes decompose on the oxidized silicon surface through the stage of forming the silicon clusters [135, 136]. The production of SiO molecules on the boundary between the silicon clusters and silicon oxide can occur only at temperatures above 700 °C. What is more, silane decomposition through the cluster nucleation stage requires that the coating of the surface by silane molecules be thick, which is achieved by subjecting the silanes in the gaseous phase to high pressures. Thick coatings bring about very high rates of silicon cluster growth immediately after cluster nucleation. This fact makes controlling their size over a 10-nm range highly problematic. So far, no decomposition of silanes on an oxidized silicon surface at gas pressures below 10^{-3} Pa has been observed [133, 135 – 138]. However, silanes can decompose under low pressures on prefabricated sections of pure silicon in windows on SiO_2 films. The selective growth of silicon in 'macroscopic' Si(001) windows creates large pyramidal islands with {113} facets on the lateral faces [133, 138]. Islands that have grown in windows of nanometer sizes have a flatter shape, with facets of various orientations [137, 139]. It should be noted that the island number density is set by the window number density, which is usually several orders of magnitude lower than in the case of deposition on oxidized silicon surfaces by the MBE method considered here. This comparison stresses the advantages of the MBE method over gas-phase deposition in fabricating nanostructures as small as 10 nm.

4.3 Causes of island stability

The energy barrier for diffusion across atomic steps (the Ehrlich – Schwoebel barrier [140 – 142]) usually determines the surface morphology in the epitaxy of metals. As germanium or silicon grows on an oxidized silicon surface, the additional barrier for diffusion is located at the boundary between the island edge and the oxide. The presence of a barrier at the island – oxide boundary makes the island thermally stable. Here, we examine the possible paths of the evolution of a surface covered with silicon islands in the presence of what remains of the silicon oxide film and in the absence of such residues, after the influx of atoms has stopped.

The decomposition of the oxide as it interacts with the silicon of the islands proceeds through the formation of volatile SiO molecules. When a continuous SiO_2 film on

silicon decomposes, this reaction begins at the film – substrate interface and continues via radial expansion of the forming pores [139, 143 – 146]. At moderate temperatures, the decomposition process is limited by the evaporation of SiO molecules, with an activation energy equal to 3.4 eV. The decomposition of silicon oxide through this mechanism proceeds with a substantial rate at temperatures higher than 700 °C and, hence, plays no noticeable role in the case at hand.

The decomposition of silicon oxide may also proceed by another mechanism, which involves the silicon adatoms. At moderate temperatures, the balance between the rate of adatom thermal generation and the rate of their incorporation determines the equilibrium concentration of adatoms on the surface. Silicon adatoms generated by the island surface may migrate to the silicon oxide through the potential barrier at the boundary between them. In the presence of adatoms, the silicon oxide decomposition follows reaction (11), i.e., at temperatures much lower than by the reaction at the film – substrate interface. However, without an external source supplying the silicon adatoms this reaction is limited by the rate at which the adatoms overcome the barrier at the island – oxide surface interface. Shibata et al. [137] found that this barrier is characterized by a high activation energy (about 3 eV) for diffusion. The barrier significantly raises the temperature of decomposition of the silicon oxide residues and, hence, restrains the spreading out of the silicon islands through the generation of adatoms.

Experimental data give evidence that pyramidal islands are retained at the silicon surface even in the absence of silicon oxide after growth at temperatures ranging from 640 to 680 °C (Figs 14c and 15) [125]. The thermal stability of pyramidal islands may be the result of the fact that the Si(113) surface possesses a stable structure [147]. The experiments conducted by Sudoh and Iwasaki [148] have shown that the equilibrium shape of silicon microcolumns is created by the {111}, {001}, and {113} faces. A characteristic feature of the Si(113) surface is the presence of a local minimum in the dependence of the surface energy on the orientation of the surface in the [110] zone (see Ref. [149]). This minimum in the surface energy for {113} explains the formation of the flat shape of the lateral faces of the pyramids, their orientation, and the stability of pyramids against their spreading out over the surface.

What makes the Si(113) surface so interesting is that it is the only thermally stable high-index face of silicon crystal. This surface is subjected to a reconstruction with the 3×2 structure [150, 151] or the 3×1 structure [152], depending on the conditions in which the reconstruction happens. The first type of reconstruction is energy-preferable at moderate temperatures. The transition to the second type occurs as the temperature rises and is completed when arriving at 500 °C [151]. At such relatively low temperatures, for processes running on the silicon surface the reverse transformation of the surface from the 3×1 reconstruction to the 3×2 reconstruction requires lowering the temperature of the sample slowly in the transition region [153]. In our case of pyramidal silicon islands with lateral {113} faces, only the 3×1 reconstruction was observed (Figs 15g – j) [125], which could be the result of rapid cooling of the sample after deposition was completed. Furthermore, the small size of the {113} facets may serve as a factor that impedes the transformation of the surface associated with the 3×2 reconstruction characterized by a larger unit cell.

As shown in Fig. 14c, the sections of the surface surrounding the pyramidal islands are covered with shallow (001) terraces consisting of a large number of atomic steps and breaks. Such surface sections generate adatoms whose concentration may be much higher than that on large atomically flat sections on which one observes a relatively rapid spreading-out of single islands [154]. It can be assumed that the high adatom concentration around the islands is a kinetic factor that hinders the smoothing-out of the surface morphology after the influx of silicon atoms has stopped.

The surface morphologies of germanium and silicon layers differ significantly when the layers grow on an oxidized silicon surface at high temperatures, i.e., when the oxide film is completely decomposed in the initial stage of growth. Here, the pyramidal silicon islands are thermally stable, while the germanium islands have a tendency to spread out, accompanied by the formation of a two-dimensional wetting layer. Such behavior agrees with the fact that the germanium surface energy is higher than that of silicon. In other words, the effect stemming from a decrease in the free surface energy in the formation of a flat silicon surface is weaker than it is for germanium in the range of coating thicknesses smaller than the critical one needed for the transition from the layer growth to the three-dimensional island growth.

4.4 Density of an island array

The density of an array of hemispherical islands depends on the amount of deposited silicon (Fig. 16). It reaches its maximum value of about 10^{13} cm^{-2} at a coating thickness of 0.7 ML at which the islands are roughly 3 nm at the base [17]. As the coating gets thicker, the density gradually decreases as a result of island coalescence. Notice that after silicon islands have formed on the surface of the silicon oxide film at 400 °C, the conditions necessary for the formation of the second layer of islands are established through oxidation of their surface in oxygen. Multiple repetition of the processes of silicon deposition with subsequent oxidation of the resulting surface creates a multilayer bulky structure of silicon islands separated by a silicon oxide film. The size of the islands and the film thickness can be controlled by selecting the proper amount of deposited silicon and the conditions of oxidation of the surface, respectively. This approach has been used to fabricate structures with an island array density in bulk amounting to about 10^{19} cm^{-3}. It is assumed that with such structures stimulated emission of light can be achieved [155].

At small silicon coating thicknesses, the nucleation mechanism determines the array density prior to island coalescence. The number density of silicon islands is practically temperature-independent in the interval extending from 400 to 590 °C (Fig. 14k), and it is nearly the same for hemispherical and pyramidal islands. The fabrication of both reaction-active states of SiO(surf) and of sections of pure silicon on the substrate, needed for the nucleation of nonepitaxial and epitaxial islands, respectively, can proceed by the following reaction

$$\mathrm{SiO_2(surf)} + \mathrm{Si(adatom)} \rightarrow \mathrm{SiO(surf)} + \mathrm{SiO(gas)}\,. \quad (13)$$

The ratio of the amounts of the SiO(surf) and SiO(gas) reaction products depends on the temperature. Here, we can use formula (10) to find the island number density, assuming that nucleation centers appear as a result of reaction (13), which is similar to reaction (7). According to formula (10), the

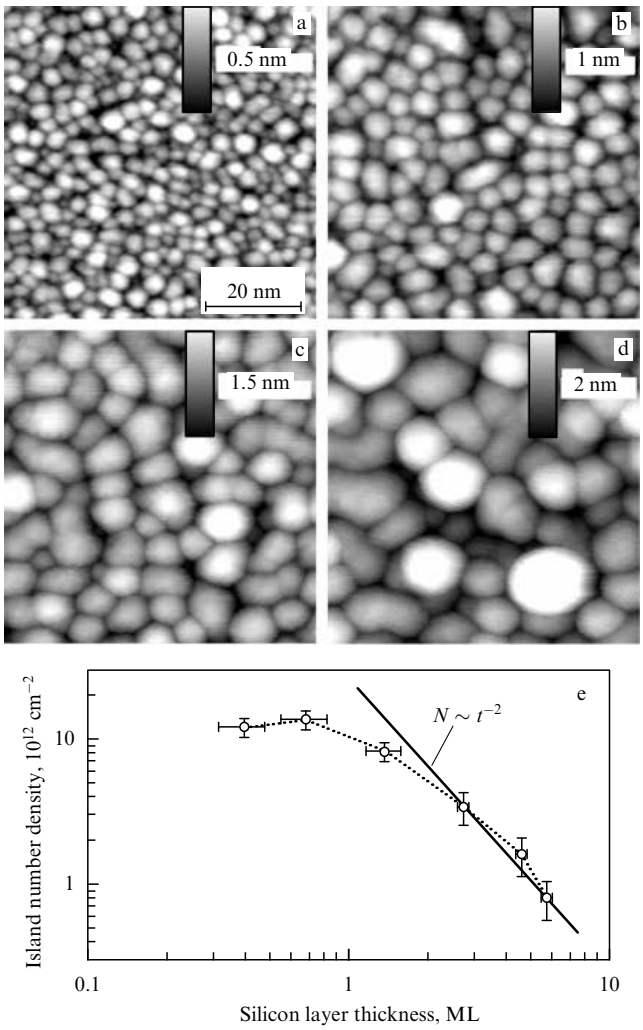

Figure 16. STM images of silicon islands grown as a result of deposition of different amounts of silicon on an oxidized Si(001) surface at 400 °C. The silicon coating thicknesses are (a) 0.7, (b) 1.4, (c) 4.6, and (d) 5.8 ML. All images depict a region with the same area: 66-by-66 nm. (e) Island array density as a function of the amount of deposited silicon. The solid line represents the approximation of the experimental data by the power function $N \sim t^{-2}$, where t is the time of deposition with a constant rate.

measured value of $N \approx 10^{13}$ cm^{-2} corresponds to the ratio $k_r^{(0)}/v \approx 3.6 \times 10^{-2}$, whose magnitude is characteristic of the reaction of single adatoms with surface atoms [107]. The difference in the values of this ratio for germanium and silicon indicates that the probability of entering silicon adatoms to the reaction with the oxide is approximately five times higher than that of germanium adatoms. Notice that Schmidt et al. [102] observed the same high island array density when certain metals were deposited on the SiO_2 surface. The researcher suggested the presence of a certain correlation in which the metals that have a greater sublimation heat at the SiO_2 surface have a higher island array density. This agrees with our data, since the silicon sublimation heat is higher than that of germanium. However, the formation of germanium and silicon islands took place at relatively moderate temperatures in the conditions of complete condensation of the deposited material. The resulting difference between germanium and silicon in this case cannot be explained by the difference in sublimation heats; instead, it is the difference in the reactivities of these elements in their reactions with silicon oxide that provides an explanation. This conclusion agrees with the data on germanium deposition on an oxidized germanium surface, which show that the island number density depends on the chemical composition of the oxide layer [156].

The island array density as a function of the growth time at the silicon deposition rate remaining constant can be obtained by assuming that all islands are of the same size and shape in each coating. The amount V of deposited silicon is given by the formula $V = wt$, where w and t are the rate and time of deposition, respectively. The deposited silicon is spent primarily on forming islands: $V = N\rho$, where ρ is the island volume. When the coating of the surface by silicon islands reaches its limit, with the surface being completely covered with islands, N becomes equal to $1/s$, where s is the island area on the surface. Since $s \sim \rho^{2/3}$ and $\rho \sim N^{-3/2}$, equaling the amounts of deposited silicon and the silicon in the island, we arrive at $wt \sim N^{-1/2}$, or $N \sim t^{-2}$. An approximation of the experimental dependence by a power function is depicted in Fig. 16e.

It should be noted that by using an oxidized silicon surface one can fabricate layers of doped silicon quantum dots in an undoped silicon matrix, provided that the doping is done during formation of three-dimensional islands and is followed by covering the islands with a layer of undoped silicon. Alternating such growth with oxidation of the surface, we can produce a multilayer structure of doped silicon quantum dots in a silicon matrix.

5. Radiative properties of germanium and silicon nanostructures

The most striking and, from the practical viewpoint, important properties of nanostructures based on semiconducting III–V compounds manifest themselves in the carrier radiative recombination [1]. Today we know in detail the radiative properties of structures consisting of germanium quantum dots in a silicon matrix, with the dots being grown in the SK regime. These structures were found to be strongly dependent on the growth temperature. For instance, structures that are fabricated at relatively low temperatures (about 400 °C) are capable of emitting photons whose energy is even lower than the width of germanium's band gap, i.e., approximately in the 0.6–0.9-eV range [157 – 159]. This is possible because germanium quantum dots in silicon form a semiconducting type-II heterostructure [160] in which the radiative recombination process involves holes trapped in the potential wells of the germanium quantum dots and electrons from the surrounding silicon, which are localized at the boundary with the germanium dots [161, 162]. The fact that germanium in silicon forms type-II heterostructures agrees with the results of electrophysical studies [91, 163, 164]. Structures grown at higher temperatures (about 600 °C) emit photons in a narrower energy range near 0.8 eV, irrespective of both the size of the germanium dots and the thickness of the silicon layers separating the germanium dot layers [165 – 169], and the reason may be that the effect of spatial quantization in the SK-grown germanium dots is weak because of their large size. The interest in structures emitting photons with an energy of about 0.8 eV arises from the use of this spectrum range in fiber-optical communication lines. However, the efficiency of optical transitions in structures with SK-grown germanium quantum dots in silicon is much lower than of those in direct-gap semiconducting III–V compounds. What

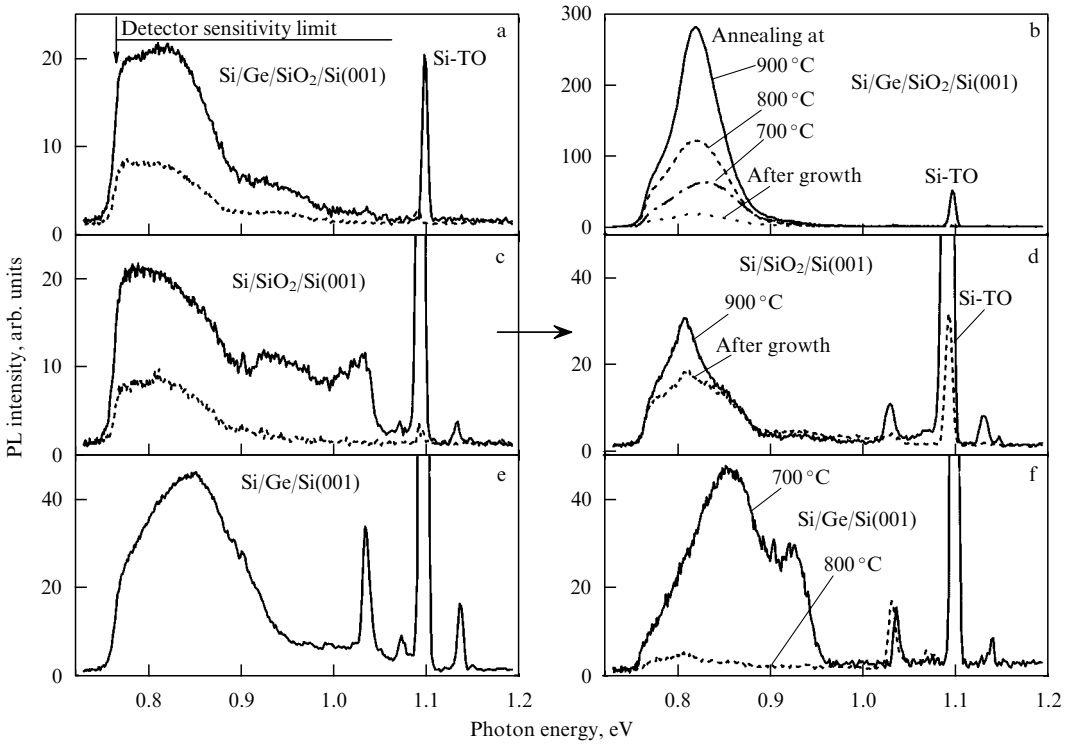

Figure 17. Photoluminescence spectra (4 K, $\lambda_{exc} = 325$ nm) of nanostructures grown (a–d) on an oxidized silicon surface as a result of deposition (a, b) of a layer of germanium islands covered with a silicon layer and (c, d) only of a silicon layer, and (e, f) in the SK regime. The spectra shown in Figs 17a, c, and d were measured before annealing. After annealing of the structures in oxygen at the indicated temperatures for 30 min, the spectra transformed into those depicted in Figs 17b, d, and f, respectively. The spectra depicted in Figs 17a and c by dotted curves correspond to structures grown at relatively low temperatures. (d) Spectra of structures grown at temperatures above 500 °C.

is more, germanium quantum dots in silicon are thermally unstable at high temperatures. Their related light emission disappears after annealings at temperatures above 700 °C. Hence, the search for new methods of fabricating Ge/Si nanostructures with high efficiencies of optical transitions and with a radiant energy in the 0.8-eV range still remain a very important goal. Let us now examine the carrier radiative recombination in germanium and silicon structures grown by utilizing oxidized silicon surfaces.

5.1 Photoluminescence of Ge/Si nanostructures grown by different methods

The photoluminescent properties of germanium layers grown on an oxidized silicon surface have been studied by different groups of researchers (see Refs [18, 101, 170, 171]). To directly compare the luminescence spectra, three types of structures were grown in a single growth chamber: in the SK regime or by depositing germanium or silicon layers on an oxidized silicon surface [18]. The layers grown on an oxidized silicon surface emit photons within a broad spectral region extending from approximately 0.75 to 1.0 eV (Figs 17a, c), while the SK-grown Ge/Si structures provide a wide photoluminescence (PL) peak with a maximum at 0.85 eV (Fig. 17e). The other distinction between these structures is that they provide a higher intensity of the Si-TO peak (band-to-band optical transitions with generation of transverse optical phonons) from the substrate. When photoluminescence is excited by the short-wave 325-nm radiation from an He–Cd laser, radiation that is absorbed by a 10-nm-thick (approximately) layer, the higher intensity of the Si-TO peak from the substrate indicates that the excited carriers migrate to a greater depth in structures with a greater crystal perfection. It should be emphasized that the PL method is applied to studying structures containing a covering silicon layer with a thickness no less than 30 nm to exclude the effect of surface states on carrier recombination in the layer of germanium quantum dots. The reduction in the intensity of the Si-TO peak is an indication that there is a large number of capture centers for the excited carriers in structures grown on an oxidized silicon surface. Their concentration increases substantially as the growth temperature drops, so that the Si-TO peak in the spectra of structures grown at low temperatures disappears.

Annealing the three types of structure leads to different changes in their PL spectra. Ge/Si structures grown on an oxidized silicon surface emit PL radiation in the 0.8-eV range with the intensity increasing by a factor of 10 to 100 as the annealing temperature rises to 1000 °C (Fig. 17b). The annealing of a structure containing only silicon layers grown at temperatures above 500 °C leads to a substantial increase in the intensity of the Si-TO peak and to retaining the weak intensity of PL in the 0.8-eV range (Fig. 17d). Ge/Si structures grown in the SK regime and annealed at temperatures above 700 °C almost completely lose the ability to emit PL radiation related to germanium quantum dots (Fig. 17f) [18, 172, 173]. Such dependence of PL on the annealing temperature is often used as a criterion for corroborating the origin of PL as related to germanium quantum dots rather than to crystal defects in the surrounding silicon. Thus, the increase in the PL intensity by a factor of 10 to 100 in the 0.8-eV range in Ge/Si structures grown on an oxidized silicon surface and annealed at temperatures above 700 °C cannot be related to germanium quantum dots; instead, it occurs because of optical recombination in the covering silicon layer. This conclusion is also supported by the absence of an

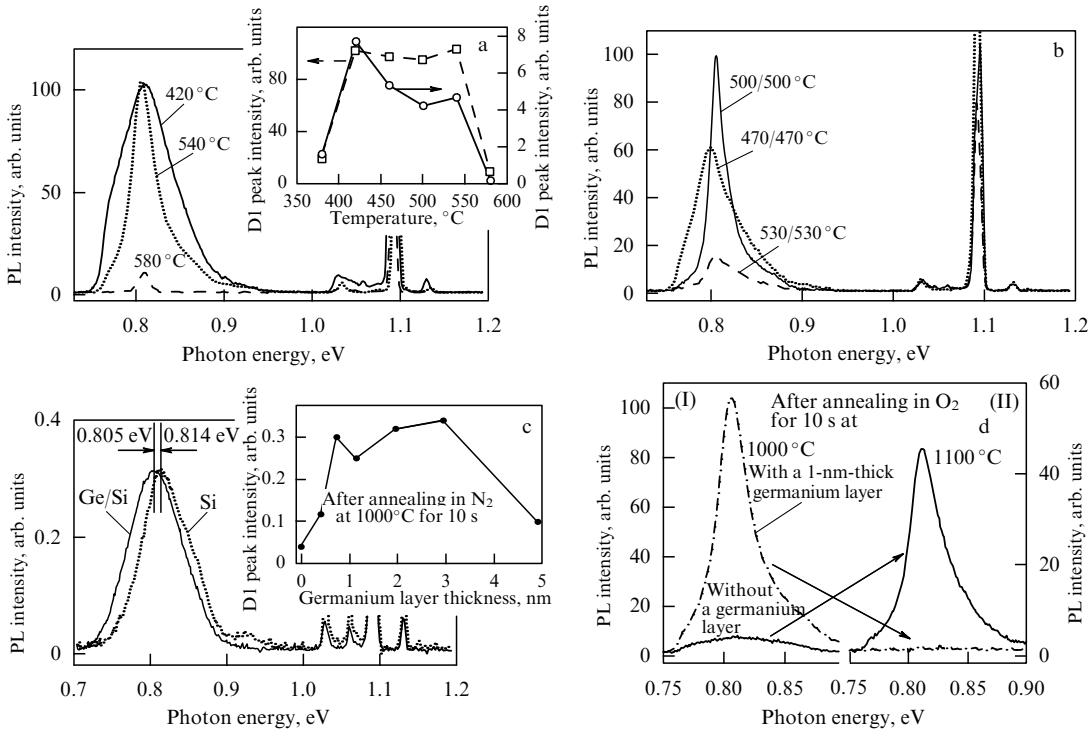

Figure 18. PL spectra (4 K, $\lambda_{exc} = 325$ nm) of nanostructured silicon layers grown in different conditions on an oxidized silicon surface. Dependence on the growth temperature (a) of germanium islands, and (b) of the covering silicon layer. (c) Dependence on the germanium layer thickness. The spectrum depicted by a dotted curve corresponds to a structure without a layer of germanium islands. The spectra (a – c) were taken after high-temperature annealing of the structures at about 1000 °C. (d) Comparison of the spectra taken after annealings at 1000 and 1100 °C.

Si-TO peak from the substrate in the PL spectra of such structures (Fig. 17b), which points to the capture of excited carriers in the covering silicon layer even before they reach the islands – Ge/Si(001) boundary.

Thus, the PL spectra in Fig. 17b demonstrate that silicon layers grown on a germanium island layer on an oxidized silicon surface are capable of emitting light only at energies in the 0.8-eV range, i.e., they have an effective width of the band gap that is much smaller than that of the silicon crystal. This is an indication that there is significant distinction between the atomic structure of these layers, which may be called layers of *nanostructured* silicon, and that of crystalline silicon. Below we shall show that layers of nanostructured Si are formed within a narrow range of the conditions of growth followed by high-temperature annealing.

5.2 Conditions necessary for the formation of nanostructured Si on a germanium island layer

PL of the highest intensity after high-temperature annealing was observed from nanostructured Si layers in which the germanium island layer had been grown at temperatures in the 400 – 540 °C range (Fig. 18a) [174]. The difference in the temperature dependences of the height of the PL peak on its integrated intensity, shown in the inset to this figure, indicates that the structures grown at higher temperatures exhibit a narrower peak in their PL spectrum. A similar dependence has also been discovered in the case where the growth temperature of the covering silicon layer is the variable parameter (Fig. 18b), the only difference being that intense PL has been observed for layers grown in a narrower temperature interval extending from 400 to 500 °C.

The other structure parameter that can be expected to strongly affect PL is the thickness of the deposited germanium or the size of the germanium islands. The results of research in this area show that within a broad range of thicknesses, approximately from 0.7 to 3 nm, neither the intensity of the PL peak nor the location of the peak on the energy scale depends on this parameter (Fig. 18c). At larger and smaller thicknesses, the PL intensity was found to be much weaker. Moreover, even structures without germanium, i.e., fabricated by depositing silicon directly on an oxidized silicon surface at temperatures in the 400 – 500 °C range, exhibited PL spectra which were close in shape, albeit with a smaller peak intensity in the 0.8-eV range. These findings confirm the previously-made inference that the intense PL in the 0.8-eV range is unrelated to carrier radiative recombination in the germanium quantum dots.

High-temperature annealing brings about a simultaneous increase in PL related to both nanostructured Si and interband transitions in the silicon substrate. The last circumstance testifies that the efficiency of radiationless recombination processes is lowered. An unexpected result is the disappearance of PL from the nanostructured Si layer after annealing at temperatures above 1000 °C for structures containing germanium island layers. In this case, the structures comprising only silicon layers grown at relatively low temperatures ranging from 400 – 500 °C emitted high-intensity PL radiation only after being annealed at 1100 °C (Fig. 18d). PL may disappear because of the diffusion of germanium atoms and their capture by the elastic stress field existing in the regions between the silicon nanocrystals, which alters the position of the energy levels.

The formation of nanostructured Si in the established growth conditions combined with subsequent high-temperature annealing may be pictured as follows. As shown in Section 3.6, within the given range of growth temperatures,

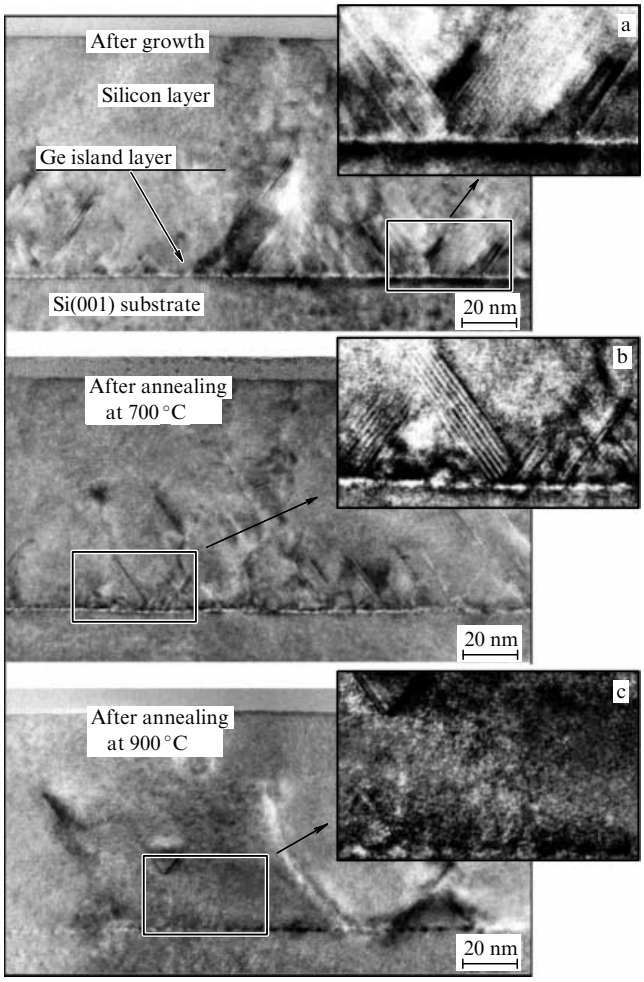

Figure 19. TEM images of a nanostructured Si layer after growth and annealing at different temperatures. The structure was fabricated by deposition of 1.0 nm of germanium on an oxidized silicon surface, followed by the deposition of 100 nm of silicon at 470 °C.

deposited silicon atoms attach themselves chiefly to germanium islands and do not, for all practical purposes, react with the oxidized silicon surface between the islands [101, 174]. The growth of three-dimensional islands continues, with the nucleus of each such island being a germanium island. The crystal structure of such islands is subjected to strong elastic strain. The coalescence of the islands accompanying subsequent growth leads to the formation of crystal defects at the boundaries between them. The presence of stacking faults in the deposited silicon layer may be observed by the appearance of additional point reflections in the HEED pattern (Fig. 13e). Figure 19a shows that the stacking faults propagate from germanium islands towards the deposited silicon layer to a depth of about several dozen nanometers. Annealing at 700 °C makes the blocks of stacking faults in the TEM images more graphic (Fig. 19b) [175]. Annealing at 900 °C leads to the formation of a more uniform structure in the entire deposited silicon layer (Fig. 19c). The identification of the system of crystal defects in nanostructured Si layers is hindered by the high concentration of the defects. Notice that high-temperature annealing does not always lead to defect propagation into the silicon substrate. Thus, nanostructured Si layers are the sections of crystalline silicon separated by sections with a system of crystal defects having a narrower effective band gap (about 0.8 eV). Such a structure is similar to the structures with quantum wells.

5.3 Ge/Si nanostructures grown at high temperatures

Ge/Si nanostructures grown on an oxidized silicon surface at temperatures from 500 to 700 °C have a crystal structure in which defects play an insignificant role. Such structures constitute the topic of research into the properties of germanium quantum dots in the silicon matrix by a variety of methods.

Milekhin et al. [114] did a comparative study of the resonant Raman scattering by strained and relaxed germanium quantum dots grown at 600 °C in the SK regime and by the method that uses the oxidation of silicon surfaces. The researchers found that there was a great difference in the positions of the peaks related to vibrations of the Ge–Ge bonds. The low-frequency shift of the peak for structures grown with the use of oxidation implies that the effect of spatial quantization of germanium dots, caused by local elastic strains, is predominant. This result agrees with the data obtained through X-ray diffraction, which show that germanium islands grown on a layer of silicon oxide over the Si(001) substrate are not subjected to elastic strains and consist entirely of germanium [96].

Dvurechensky et al. [176] established that the electron transport in a layer of germanium quantum dots in a silicon matrix that had been grown at 650 °C is achieved by the hopping mechanism. Here, the hole-capture cross section measured as a function of the depth of the energy levels has a value that is several orders of magnitude greater than the values known from earlier studies of silicon-based structures. The researchers revealed that layers of germanium quantum dots might be used to fabricate photodetectors capable of operating in the near and medium infrared (IR) ranges.

Such properties as the dome shape and small size of germanium islands grown with the use of oxidation of a silicon surface bring the islands as close as possible to quantum dots of zero dimension. These properties have made it possible to study the Stark effect for type-II heterostructures. The strong influence that the Stark effect has on the photoconductivity stems from the large magnitude of the dipole moment of the excitons and is the result of the spatial separation of electrons and holes in type-II heterostructures. The Stark effect is characterized by the emergence of two peaks in the photoconduction spectrum caused by the formation of two configurations of dipoles with opposite directions in relation to the applied electric field and, therefore, affected very differently by this field [91].

The amount of silicon oxide film remaining in the structure depends on the temperature at which germanium is deposited. Nakayama et al. [177] showed that the quantizing energy levels are determined not only by the size of the quantum dot but also by the potential barrier generated by the residues of the silicon oxide film. The researchers believe that the possibility of changing this barrier is an additional parameter for controlling the energy levels in the germanium quantum dots. The quantizing levels in germanium dots grown on an oxidized silicon surface have also been studied by scanning tunnel spectroscopy [178] and the photoelectron spectroscopy [179] methods. It was found that as the size of germanium dots decreases from 7 to 2 nm, their band gap increases by 1.4 eV, in accordance with the semiempirical calculations for the spherical quantum dot model.

5.4 Nanostructured Si layers grown on an oxidized silicon surface

The conditions necessary for the formation of a nanostructured Si layer on germanium island arrays point to the theoretical possibility of fabricating such a layer by depositing silicon directly on an oxidized silicon surface. Such a possibility emerges because of the initial stage in the growth of silicon on the oxidized surface, the stage which proceeds by the same mechanism as it does for germanium growth. Experiments have revealed that silicon layers grown on an oxidized silicon surface are capable of emitting intensive PL radiation, but only after annealing the sample at higher temperatures, 1000 – 1100 °C (Fig. 20a) [180]. As shown in Section 4, the nucleation of three-dimensional silicon islands occurs either epitaxially or nonepitaxially in relation to the substrate within a broad temperature range. As growth continues, the sections of silicon with a high concentration of stacking faults appear at the island intergrowth boundaries. The number of defects depends on the epitaxial-to-nonepitaxial island ratio, which is determined by the temperature of the initial stage of growth. The results of experiments in which only the deposition temperature of the first 2 nm of silicon was varied, while subsequent growth took place at a fixed temperature, are presented in Fig. 20b. The silicon layers grown at temperatures ranging from 400 to 500 °C exhibited the emission of the most intensive PL radiation after annealing. Silicon layers were fabricated that produced PL radiation whose intensity was even higher than that of layers grown with the use of germanium islands. The character of the temperature dependences indicates that both types of structures emit PL radiation in the 0.8-eV range at room temperature (Fig. 20d). Notice that the PL intensity decreases by a factor of approximately 1000 as the sample temperature rises from 4 to 295 K. The shift of the PL peak to a lower-energy region with increasing temperature (Fig. 20c) is caused by the temperature narrowing of the silicon's band gap.

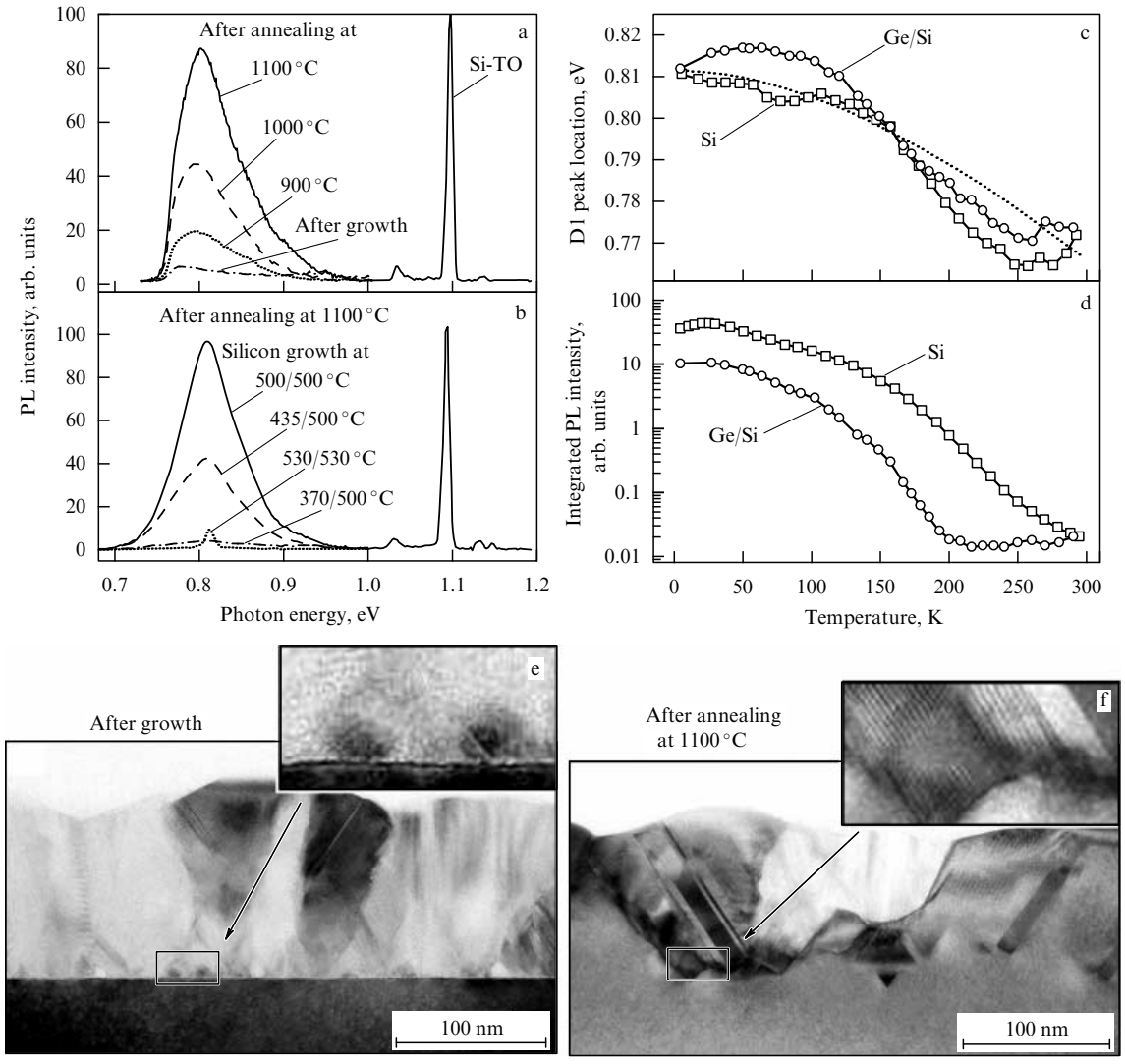

Figure 20. PL spectra (4 K, $\lambda_{exc} = 325$ nm) of nanostructured Si layers grown in two stages (a) (2 nm at $T_1 = 450$ °C, and 100 nm at $T_2 = 500$ °C) on an oxidized silicon surface after annealing at different temperatures, and (b) presented as a dependence on the growth temperature in the initial stage (the growth temperatures T_1/T_2 are listed in the figure). The temperature dependences (c) of the position of the peak at 0.8 eV, and (d) the integrated PL intensity for layers of nanostructured Si grown directly on the oxidized silicon surface (Si) and on an array of germanium islands (Ge/Si). The dotted curve represents the calculated temperature dependence for $E_g - 0.36$ eV, where E_g is the silicon band gap. (e, f) TEM images of a nanostructured Si layer grown on an oxidized silicon surface in two stages (2 nm at $T_1 = 430$ °C, and 100 nm at $T_2 = 500$ °C) before (e) and after (f) annealing in an oxygen atmosphere for several seconds.

TEM images show that there is a system of stacking faults in a silicon layer grown on an oxidized silicon surface at moderate temperatures (Figs 20e, f). What is interesting here is that the high concentration of these defects spreads from the boundary with the substrate to the entire deposited layer. High-temperature annealing creates a better-ordered arrangement of the defects in the deposited silicon layer and does not result in their spreading to the substrate.

Although the origin of silicon PL in an energy range much narrower than the band gap has been studied for nearly three decades [181 – 185], the relation between the energy levels generated by the crystal defects and the optical-transition diagram has yet to be fully established. On the one hand, the reason for this situation lies in the complexity of theoretical examinations of the silicon structures that contain different configurations of atoms in the defects. Such calculations usually produce several energy levels in the silicon band gap. On the other hand, such experimental methods as, say, deep level transient spectroscopy also show the presence of several energy levels, even in structures with one type of defects dominating. Here, the radiative recombination of carriers involves only some of these levels. It has been established, both theoretically and experimentally, that such thermally stable defects as dislocations generate shallow levels located near the edge of the valence band [186, 187], levels that cannot by themselves guarantee radiative recombination with an energy of 0.8 eV. Another thermally stable type of defects comprises clusters with an interstitial silicon atom. According to calculations, such defects generate deep energy levels in the silicon band gap and, in principle, can by themselves provide transitions with an energy of 0.8 eV [188]. Earlier researchers analyzed the temperature dependence of the PL intensity and concluded that radiation emission in the 0.8-eV range is the result of optical transitions between a shallow level near the edge of the valence band and a deep level [189], probably related to an interstitial silicon atom.

The low efficiency of light emission by silicon is due to its nondirect gap electronic structure. The breaking of the crystal's symmetry as a result of defects that appear in the crystal introduces a factor of spatial indeterminacy and, therefore, reduces the extent to which direct optical transitions are forbidden (this exclusion principle follows from the momentum conservation law). Most vividly this factor acts as the crystal size decreases because of spatial quantization, whose effect manifests itself in such nanostructures as porous silicon and crystal silicon clusters introduced into various wide-gap materials [190 – 194]. These structures emit visible light. As a result of allowing for direct optical transitions, the efficiency of emission changes dramatically, reaching values comparable to the efficiency of emission by direct gap semiconductors [195, 196].

The presence of defects in nanostructured Si layers and PL data make it possible to think of nanostructured Si as a material consisting of clusters of crystal silicon separated by the sections with a system of crystal defects. Here, the sections with defects have an electronic structure with an effective band gap of about 0.8 eV and may be interpreted as quantum wells in silicon. The data from PL measurements show that excited carriers are localized in these quantum wells, which leads to radiative recombination only with an energy in the 0.8-eV range and with an efficiency much higher than that for crystal silicon. Probably, this occurs because of initiating direct optical transitions. This property makes nanostructured Si material similar to other silicon nanostructures, the only difference being that nanostructured Si emits IR radiation.

So far, the study of the IR emission in the 1.5 – 1.6-μm range by silicon-based materials has focused mainly on Er-containing structures [197 – 199]. The excitation of Er ions in silicon occurs as a result of inelastic collisions with high-energy electrons in diode structures operating at elevated voltages. The radiative properties of nanostructured Si layers and the conditions needed for fabricating such structures point to the potential of this material as an alternative to various structures based on the Si – Er system for building light sources in the near-IR spectral range.

6. Conclusion

In the course of heteroepitaxy of germanium on silicon, nucleation of three-dimensional islands in the supersaturated layer of adatoms on the surface of the elastically strained germanium wetting layer occurs. The islands spontaneously grow after nucleation because of absorption of the adatom layer and a fraction of the strained wetting layer, which makes the layer thinner. As a result, on the Si(111) surface the germanium islands form with sizes of about 50 nm at their base with a rarefied density of the array of order 10^{10} cm^{-2}.

Oxidation of the silicon surface leads to a dramatic change in the mechanism of the subsequent growth of germanium and silicon. Three-dimensional islands form without a wetting layer with an ultimately high array density of $10^{12} - 10^{13}$ cm^{-2} and a size less than 10 nm at the base, which is determined solely by the amount of the deposited material. The mechanism of island nucleation consists of the direct interaction between a single deposited atom and the surface, with insignificant mechanical stresses. In structures fabricated on the basis of such islands, spatial quantization effects play a dominant role. Moreover, layers of germanium or silicon islands grown on an oxidized silicon surface at 400 – 500 °C establish unique conditions for the formation of nanostructured Si layers on them, which after high-temperature annealing are capable of efficiently emitting photons with wavelengths in the 1.5 – 1.6-μm range. This property and the conditions needed for fabricating layers show their potential in the fabrication of IR light sources by the traditional methods of silicon technology.

References

1. Ledentsov N N et al. *Fiz. Tekh. Poluprovodn.* **32** 385 (1998) [*Semicond.* **32** 343 (1998)]
2. Pchelyakov O P et al. *Fiz. Tekh. Poluprovod.* **34** 1281 (2000) [*Semicond.* **34** 1229 (2000)]
3. Bimberg D, Grundmann M, Ledentsov N N *Quantum Dot Heterostructures* (Toronto: John Wiley & Sons, 2001)
4. Yakimov A I, Dvurechenskii A V, Nikiforov A I, in *Handbook of Semiconductor Nanostructures and Nanodevices* Vol. 1 (Nanotechnology Book Ser., Vol. 4, Eds A A Balandin, K L Wang) (Stevenson Ranch, Calif.: Am. Sci. Publ., 2006) Ch. 2
5. Kukushkin S A, Osipov A V *Usp. Fiz. Nauk* **168** 1083 (1998) [*Phys. Usp.* **41** 983 (1998)]
6. Brunner K *Rep. Prog. Phys.* **65** 27 (2002)
7. Mo Y-W et al. *Phys. Rev. Lett.* **65** 1020 (1990)
8. Yakimov A I et al. *Appl. Phys. Lett.* **75** 1413 (1999)
9. Schmidt O G et al. *Appl. Phys. Lett.* **71** 2340 (1997)
10. Peng C S et al. *Phys. Rev. B* **57** 8805 (1998)
11. Shklyaev A A, Shibata M, Ichikawa M *Phys. Rev. B* **62** 1540 (2000)
12. Sakamoto T et al. *Appl. Phys. Lett.* **47** 617 (1985)
13. Mo Y-W et al. *Phys. Rev. Lett.* **63** 2393 (1989)

14. Latyshev A V, Aseev A L *Monoatomnye Stupeni na Poverkhnosti Kremniya* (Monatomic Steps on a Silicon Surface) (Novosibirsk: Izd. SO RAN, 2006)
15. Gossmann H-J, Schubert E F *CRC Crit. Rev. Solid State Mater.* **18** 1 (1993)
16. Lifshits V G, Repinskii S M *Protsessy na Poverkhnosti Tverdykh Tel* (Processes on the Solid Surfaces) (Vladivostok: Dal'nauka, 2003)
17. Shklyaev A A, Ichikawa M *Phys. Rev. B* **65** 045307 (2001)
18. Shklyaev A A et al. *Appl. Phys. Lett.* **88** 121919 (2006)
19. Asai M, Ueba H, Tatsuyama C *J. Appl. Phys.* **58** 2577 (1985)
20. Marée P M J et al. *Surf. Sci.* **191** 305 (1987)
21. Eaglesham D J, Cerullo M *Phys. Rev. Lett.* **64** 1943 (1990)
22. Köhler U et al. *Surf. Sci.* **248** 321 (1991)
23. Snyder C W et al. *Phys. Rev. Lett.* **66** 3032 (1991)
24. Leonard D et al. *Appl. Phys. Lett.* **63** 3203 (1993)
25. LeGoues F K et al. *Surf. Sci.* **349** 249 (1996)
26. Xie Q et al. *Phys. Rev. Lett.* **75** 2542 (1995)
27. Tersoff J, Teichert C, Lagally M G *Phys. Rev. Lett.* **76** 1675 (1996)
28. Voigtländer B, Zinner A *Appl. Phys. Lett.* **63** 3055 (1993)
29. Goryll M et al. *Appl. Phys. Lett.* **71** 410 (1997)
30. Ansari Z A, Arai T, Tomitori M *Surf. Sci.* **574** L17 (2005)
31. Ratto F et al. *Phys. Rev. Lett.* **96** 096103 (2006)
32. Tomitori M et al. *Surf. Sci.* **301** 214 (1994)
33. Omi H, Ogino T *Appl. Phys. Lett.* **71** 2163 (1997)
34. Shklyaev A A, Shibata M, Ichikawa M *Surf. Sci.* **416** 192 (1998)
35. Tersoff J, LeGoues F K *Phys. Rev. Lett.* **72** 3570 (1994)
36. Shchukin V A, Bimberg D *Rev. Mod. Phys.* **71** 1125 (1999)
37. Brunner K *Rep. Prog. Phys.* **65** 27 (2002)
38. Stoyanov S, Kashchiev D, in *Current Topics in Materials Science* Vol. 7 (Ed. E Kaldis) (Amsterdam: North-Holland, 1981) p. 69
39. Zangwill A, in *Evolution of Surface and Thin Film Microstructure* (MRS Symp. Proc., Vol. 280, Eds H A Atwater et al.) (Pittsburgh, Pa.: MRS, 1993) p. 121
40. Venables J A *Surf. Sci.* **299/300** 798 (1994)
41. Markov I *Phys. Rev. B* **56** 12544 (1997)
42. Shklyaev A A, Ichikawa M, in *Handbook of Semiconductor Nanostructures and Nanodevices* Vol. 1 (Nanotechnology Book Ser., Vol. 4, Eds A A Balandin, K L Wang) (Stevenson Ranch, Calif.: Am. Sci. Publ., 2006) Ch. 8
43. Zuo J-K et al. *Phys. Rev. Lett.* **72** 3064 (1994)
44. Amar J G, Family F *Thin Solid Films* **272** 208 (1996)
45. Shklyaev A A, Aono M, Suzuki T *Surf. Sci.* **423** 61 (1999)
46. Shklyaev A A, Shibata M, Ichikawa M *Phys. Rev. B* **58** 15647 (1998)
47. Voigtländer B et al. *Phys. Rev. B* **51** 7583 (1995)
48. Rauscher H, Braun J, Behm R J *Phys. Rev. Lett.* **96** 116101 (2006)
49. Selloni A, Takeuchi N, Tosatti E *Surf. Sci.* **331 – 333** 995 (1995)
50. Allen F G *J. Phys. Chem. Solids* **19** 87 (1961)
51. Arthur J R *J. Phys. Chem. Solids* **25** 583 (1964)
52. Shklyaev A A, Repinskii S M *Fiz. Tekh. Poluprovodn.* **14** 1300 (1980)
53. Spencer B J, Tersoff J *Phys. Rev. Lett.* **79** 4858 (1997)
54. LeGoues F K et al. *Phys. Rev. B* **44** 12894 (1991)
55. Minoda H et al. *Surf. Sci.* **357 – 358** 418 (1996)
56. Shklyaev A A, Shibata M, Ichikawa M *Thin Solid Films* **343 – 344** 532 (1999)
57. Zinke-Allmang M, Feldman L C, Grabow M H *Surf. Sci. Rep.* **16** 377 (1992)
58. Deelman P W, Thundat T, Schowalter L J *Appl. Surf. Sci.* **104/105** 510 (1996)
59. Bolkhovityanov Yu B, Pchelyakov O P, Chikichev S I *Usp. Fiz. Nauk* **171** 689 (2001) [*Phys. Usp.* **44** 655 (2001)]
60. Osipov A V et al. *Phys. Rev. B* **64** 205421 (2001)
61. Shklyaev A A, Shibata M, Ichikawa M *J. Vac. Sci. Technol. B* **19** 103 (2001)
62. Shklyaev A A, Ichikawa M *Usp. Fiz. Nauk* **176** 913 (2006) [*Phys. Usp.* **49** 887 (2006)]
63. Vescan L *J. Phys.: Condens. Matter* **14** 8235 (2002)
64. Gossmann H-J, Feldman L C, Gibson W M *Surf. Sci.* **155** 413 (1985)
65. Hammar M et al. *Surf. Sci.* **349** 129 (1996)
66. Sakamoto K et al. *Jpn. J. Appl. Phys.* **26** 666 (1987)
67. Miki K, Sakamoto K, Sakamoto T *Mater. Res. Soc. Symp. Proc.* **148** 323 (1989)
68. Osipov A V et al. *Appl. Surf. Sci.* **188** 156 (2002)
69. Goldfarb I, Banks-Sills L, Eliasi R *Phys. Rev. Lett.* **97** 206101 (2006)
70. Müller P, Saúl A *Surf. Sci. Rep.* **54** 157 (2004)
71. Latyshev A V et al. *Surf. Sci.* **213** 157 (1989)
72. Shibata M, Shklyaev A A, Ichikawa M *J. Electron Microsc.* **49** 217 (2000)
73. Latyshev A V, Krasilnikov A B, Aseev A L *Surf. Sci.* **311** 395 (1994)
74. Ogino T, Hibino H, Hommal Y *Jpn. J. Appl. Phys.* **34** L668 (1995)
75. Ogino T et al. *Surf. Sci.* **514** 1 (2002)
76. Zhang Z et al. *Surf. Sci.* **497** 93 (2002)
77. Shklyaev A A, Shibata M, Ichikawa M *Appl. Phys. Lett.* **72** 320 (1998)
78. Fujita S et al. *Appl. Phys. Lett.* **69** 638 (1996)
79. Fujita S et al. *J. Vac. Sci. Technol. A* **15** 1493 (1997)
80. Watanabe H, Ichikawa M *Rev. Sci. Instrum.* **67** 4185 (1996)
81. Shklyaev A A, Ichikawa M *J. Vac. Sci. Technol. B* **24** 739 (2006)
82. Horn-von Hoegen M et al. *Phys. Rev. B* **49** 2637 (1994)
83. Peng C S et al. *Phys. Rev. B* **57** 8805 (1998)
84. Schmidt O G et al. *Appl. Phys. Lett.* **71** 2340 (1997)
85. Butz R, Lüth H *Thin Solid Films* **336** 69 (1998)
86. Kim J Y et al. *Thin Solid Films* **369** 96 (2000)
87. Yoo K, Zhang Z, Wendelken J F *Jpn. J. Appl. Phys.* **42** L1232 (2003)
88. Li A P et al. *Phys. Rev. B* **69** 245310 (2004)
89. Wang L et al. *Nanotechnology* **13** 714 (2002)
90. Kolobov A V et al. *Appl. Phys. Lett.* **78** 2563 (2001)
91. Yakimov A I et al. *Phys. Rev. B* **67** 125318 (2003)
92. Kanjilal A et al. *Appl. Phys. Lett.* **82** 1212 (2003)
93. Li Q et al. *Appl. Phys. Lett.* **83** 5032 (2003)
94. Nikiforov A I et al. *Fiz. Tverd. Tela* **46** 80 (2004) [*Phys. Solid State* **46** 77 (2004)]
95. Barski A et al. *Appl. Phys. Lett.* **77** 3541 (2000)
96. Derivaz M et al. *Appl. Phys. Lett.* **84** 3295 (2004)
97. Shimizu N et al. *Ultramicroscopy* **18** 453 (1985)
98. Kosolobov S S, Aseev A L, Latyshev A V *Fiz. Tekh. Poluprovodn.* **35** 1084 (2001) [*Semicond.* **35** 1038 (2001)]
99. Shklyaev A A, Suzuki T *Surf. Sci.* **351** 64 (1996)
100. Frantsuzov A A, Makrushin N I *Surf. Sci.* **40** 320 (1973)
101. Shklyaev A A, Ichikawa M *Surf. Sci.* **514** 19 (2002)
102. Schmidt A A et al. *Surf. Sci.* **349** 301 (1996)
103. Fujita K, Watanabe H, Ichikawa M *J. Cryst. Growth* **188** 197 (1998)
104. Johnson K E, Engel T *Phys. Rev. Lett.* **69** 339 (1992)
105. Chambliss D D, Johnson K E *Phys. Rev. B* **50** 5012 (1994)
106. Zinke-Allmang M *Thin Solid Films* **346** 1 (1999)
107. Weinberg W H, in *Kinetics of Interface Reactions* (Springer Series in Surface Sciences, Vol. 8, Eds M Grunze, H J Kreuzer) (New York: Springer-Verlag, 1987) p. 94
108. Frankl D R, Venables J A *Adv. Phys.* **19** 409 (1970)
109. Campbell C T *Surf. Sci. Rep.* **27** 1 (1997)
110. Kolobov A V et al. *J. Vac. Sci. Technol. À* **20** 1116 (2002)
111. Kolobov A V et al. *Nucl. Instrum. Meth. Phys. Res. B* **199** 174 (2003)
112. Wei S et al. *J. Appl. Phys.* **82** 4810 (1997)
113. Kolobov A V *J. Appl. Phys.* **87** 2926 (2000)
114. Milekhin A G et al. *Fiz. Tverd. Tela* **46** 94 (2004) [*Phys. Solid State* **46** 92 (2004)]
115. Boscherini F et al. *Appl. Phys. Lett.* **76** 682 (2000)
116. Ratto F et al. *Appl. Phys. Lett.* **84** 4526 (2004)
117. Migas D B et al. *Phys. Rev. B* **69** 235318 (2004)
118. Kolobov A V et al. *Appl. Phys. Lett.* **81** 3855 (2002)
119. Volodin V A et al. *Fiz. Tekh. Poluprovodn.* **37** 1220 (2003) [*Semicond.* **37** 1190 (2003)]
120. Fonseca A et al. *Nucl. Instrum. Meth. Phys. Res. B* **249** 462 (2006)
121. Sutter P, Lagally M G *Phys. Rev. Lett.* **81** 3471 (1998)
122. Chaparro S A, Zhang Y, Drucker J *Appl. Phys. Lett.* **76** 3534 (2000)
123. Kamins T I et al. *Appl. Phys. A* **67** 727 (1998)
124. Lang C et al. *Phys. Rev. Lett.* **97** 226104 (2006)
125. Shklyaev A A, Zielasek V *Surf. Sci.* **541** 234 (2003)
126. Saranin A A et al. *Appl. Surf. Sci.* **243** 199 (2005)
127. Ohkubo K et al. *Surf. Sci.* **260** 44 (1992)
128. Shklyaev A A, Aono M, Suzuki T *Phys. Rev. B* **54** 10890 (1996)
129. Raschke M B, Bratu P, Höfer U *Surf. Sci.* **410** 351 (1998)
130. Ol'shanetskii B Z, Repinskii S M, Shklyaev A A *Pis'ma Zh. Eksp. Teor. Fiz.* **25** 195 (1977) [*JETP Lett.* **25** 178 (1977)]
131. Olshanetsky B Z, Shklyaev A A *Surf. Sci.* **82** 445 (1979)
132. Olshanetsky B Z, Mashanov V I *Surf. Sci.* **111** 414 (1981)
133. Vescan L, Grimm K, Dieker C *J. Vac. Sci. Technol. B* **16** 1549 (1998)

134. Shibata M et al. *J. Cryst. Growth* **220** 449 (2000)
135. Kruchinin V N, Repinskii S M, Shklyaev A A *Poverkhnost'* (3) 60 (1987)
136. Kruchinin V N, Repinsky S M, Shklyaev A A *Surf. Sci.* **275** 433 (1992)
137. Shibata M et al. *Phys. Rev. B* **61** 7499 (2000)
138. Hirayama H, Hiroi M, Ide T *Phys. Rev. B* **48** 17331 (1993)
139. Fujita K, Watanabe H, Ichikawa M *Appl. Phys. Lett.* **70** 2807 (1997)
140. Ehrlich G, Hudda F G *J. Chem. Phys.* **44** 1039 (1966)
141. Schwoebel R L, Shipsey E J *J. Appl. Phys.* **37** 3682 (1966)
142. Schwoebel R L *J. Appl. Phys.* **40** 614 (1969)
143. Frantsuzov A A, Makrushin N I *Zh. Tekh. Fiz.* **45** 600 (1975) [*Sov. Phys. Tech. Phys.* **20** 372 (1975)]
144. Frantsuzov A A, Makrushin N I *Thin Solid Films* **32** 247 (1976)
145. Tromp R et al. *Phys. Rev. Lett.* **55** 2332 (1985)
146. Rubloff G W *J. Vac. Sci. Technol. A* **8** 1857 (1990)
147. Eaglesham D J et al. *Phys. Rev. Lett.* **70** 1643 (1993)
148. Sudoh K, Iwasaki H *Phys. Rev. Lett.* **87** 216103 (2001)
149. Bermond J M et al. *Surf. Sci.* **330** 48 (1995)
150. Myler U, Jacobi K *Surf. Sci.* **220** 353 (1989)
151. Schreiner J, Jacobi K, Selke W *Phys. Rev. B* **49** 2706 (1994)
152. Olshanetsky B Z et al. *Surf. Sci.* **306** 327 (1994)
153. Dabrowski J, Müssig H J, Wolff G *Phys. Rev. Lett.* **73** 1660 (1994)
154. Ichimiya A, Tanaka Y, Ishiyama K *Phys. Rev. Lett.* **76** 4721 (1996)
155. Pavesi L et al. *Nature* **408** 440 (2000)
156. Nakamura Y et al. *J. Appl. Phys.* **95** 5014 (2004)
157. Vostokov N V et al. *Pis'ma Zh. Eksp. Teor. Fiz.* **76** 425 (2002) [*JETP Lett.* **76** 365 (2002)]
158. Denker U et al. *Appl. Phys. Lett.* **82** 454 (2003)
159. Novikov A V et al. *Physica E* **16** 467 (2003)
160. Yu P Y, Cardona M *Fundamentals of Semiconductors: Physics and Materials Properties* (Berlin: Springer-Verlag, 1996)
161. Fukatsu S et al. *Appl. Phys. Lett.* **71** 258 (1997)
162. Eberl K et al. *Thin Solid Films* **369** 33 (2000)
163. Dvurechenskii A V, Yakimov A I *Fiz. Tekh. Poluprovodn.* **35** 1143 (2001) [*Semicond.* **35** 1095 (2001)]
164. Yakimov A I et al. *Phys. Rev. B* **63** 045312 (2001)
165. Yam V et al. *Thin Solid Films* **380** 78 (2000)
166. Sunamura H et al. *Appl. Phys. Lett.* **66** 3024 (1995)
167. Palange E et al. *Appl. Phys. Lett.* **68** 2982 (1996)
168. Schmidt O G et al. *Appl. Phys. Lett.* **77** 2509 (2000)
169. Dunbar A et al. *Appl. Phys. Lett.* **78** 1658 (2001)
170. Shamirzaev T S et al. *Fiz. Tverd. Tela* **47** 80 (2005) [*Phys. Solid State* **47** 82 (2005)]
171. Fonseca A et al. *Mat. Sci. Eng. B* **124–125** 462 (2005)
172. Dashiell M W, Denker U, Schmidt O G *Appl. Phys. Lett.* **79** 2261 (2001)
173. Konle J, Presting H, Kibbel H *Physica E* **16** 596 (2003)
174. Shklyaev A A, Ichikawa M *Appl. Phys. Lett.* **80** 1432 (2002)
175. Shklyaev A A et al. *J. Phys.: Condens. Matter* **19** 136004 (2007)
176. Dvurechensky A V et al. *Fiz. Nizk. Temp.* **30** 1169 (2004) [*Low Temp. Phys.* **30** 877 (2004)]
177. Nakayama Y et al. *Appl. Phys. Lett.* **88** 253102 (2006)
178. Nakamura Y et al. *Appl. Phys. Lett.* **87** 133119 (2005)
179. Konchenko A et al. *Phys. Rev. B* **73** 113311 (2006)
180. Shklyaev A A, Nakamura Y, Ichikawa M *J. Appl. Phys.* **101** 033532 (2007)
181. Drozdov N A, Patrin A A, Tkachev V D *Pis'ma Zh. Eksp. Teor. Fiz.* **23** 651 (1976) [*JETP Lett.* **23** 597 (1976)]
182. Kveder V V et al. *Phys. Rev. B* **51** 10520 (1995)
183. Leoni E et al. *Eur. Phys. J. Appl. Phys.* **27** 123 (2004)
184. Kittler M et al. *Phys. Status Solidi A* **203** 802 (2006)
185. Kveder V et al. *Phys. Status Solidi A* **202** 901 (2005)
186. Liu F et al. *Phys. Rev. B* **51** 17192 (1995)
187. Castaldini A et al. *Phys. Rev. Lett.* **95** 076401 (2005)
188. Blumenau A T et al. *Phys. Rev. Lett.* **87** 187404 (2001)
189. Suezawa M, Sasaki Y, Sumino K *Phys. Status Solidi A* **79** 173 (1983)
190. Landsberg P T *Solid-State Electron.* **10** 513 (1967)
191. Canham L T *Appl. Phys. Lett.* **57** 1046 (1990)
192. Takagahara T, Takeda K *Phys. Rev. B* **46** 15578 (1992)
193. Kovalev D et al. *Phys. Status Solidi B* **215** 871 (1999)
194. Feng D H et al. *Phys. Rev. B* **68** 035334 (2003)
195. Cullis A G, Canham L T, Calcott P D J *J. Appl. Phys.* **82** 909 (1997)
196. Tsybeskov L et al. *Appl. Phys. Lett.* **72** 43 (1998)
197. Franzò G et al. *Appl. Phys. Lett.* **64** 2235 (1994)
198. Remizov D Yu et al. *Fiz. Tverd. Tela* **47** 95 (2005) [*Phys. Solid State* **47** 98 (2005)]
199. Kenyon A J *Semicond. Sci. Technol.* **20** R65 (2005)